Continuum mechanics in cardiovascular engineering and biology

Prof. Stéphane AVRIL

MINES SAINT-ETIENNE
First Grande Ecole
outside Paris
Founded in 1816

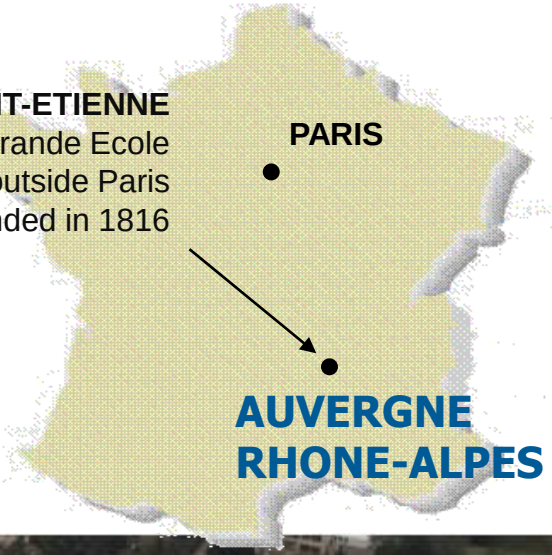

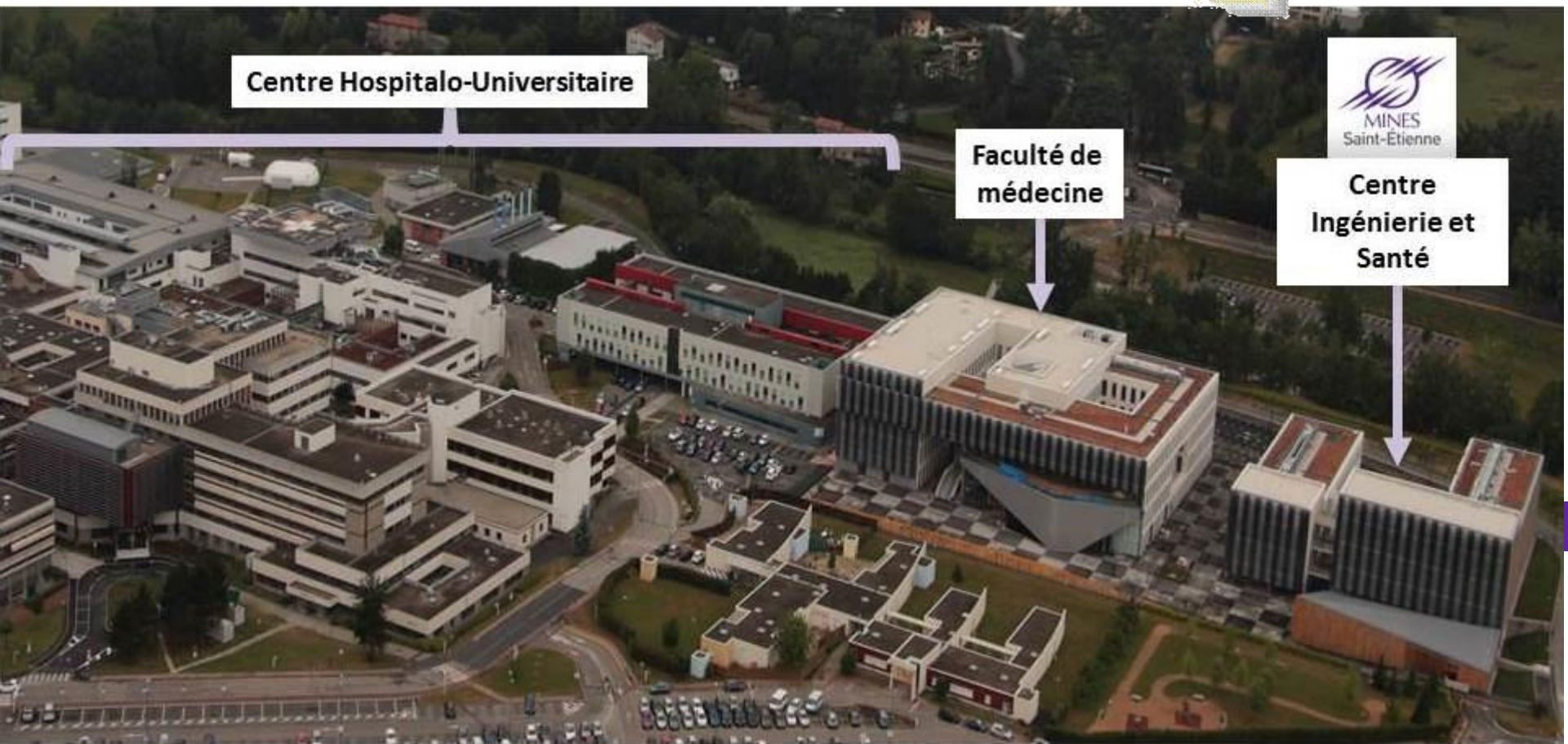

Computational mechanics in the OR for vascular surgery?

www.predisurge.com

Arterial biomechanics and mechanobiology – Position of photomechanics

Schematic representation of aortic structure

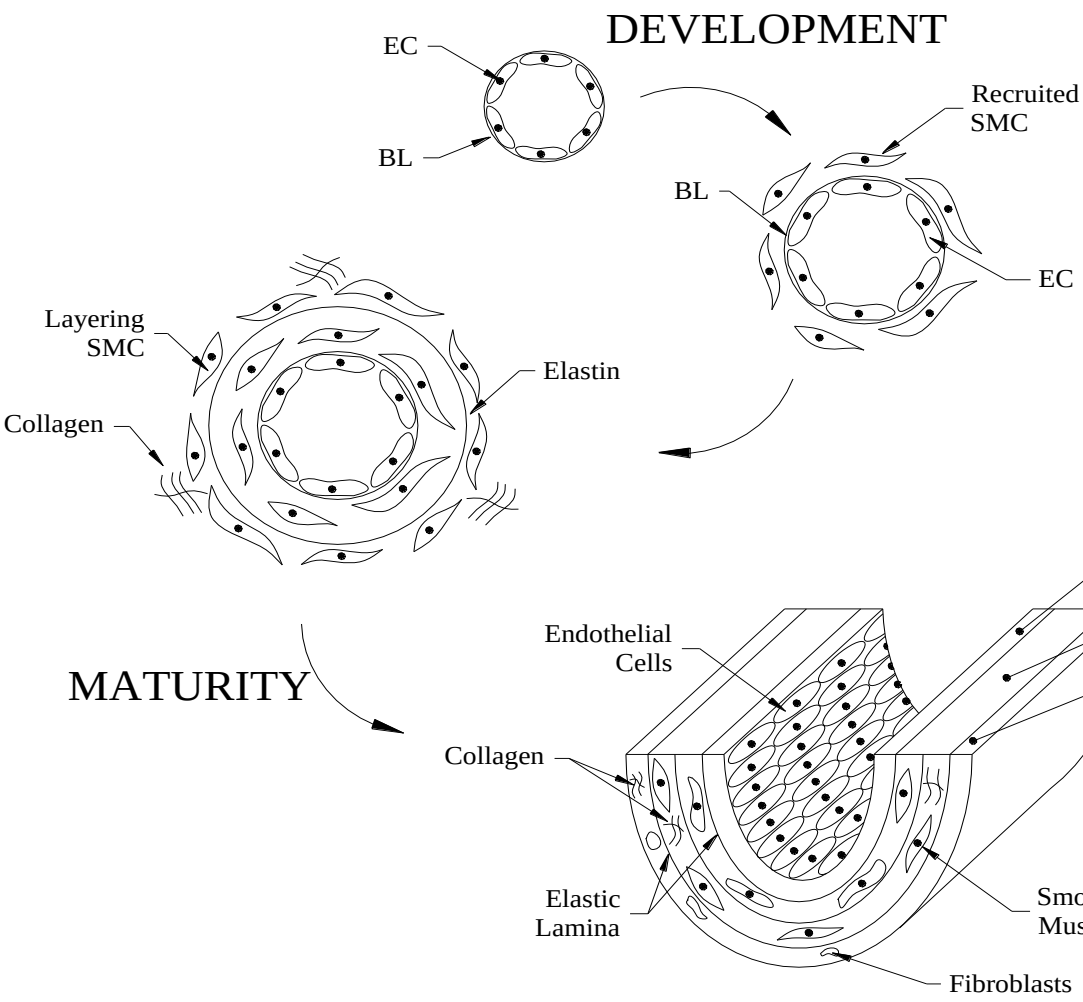

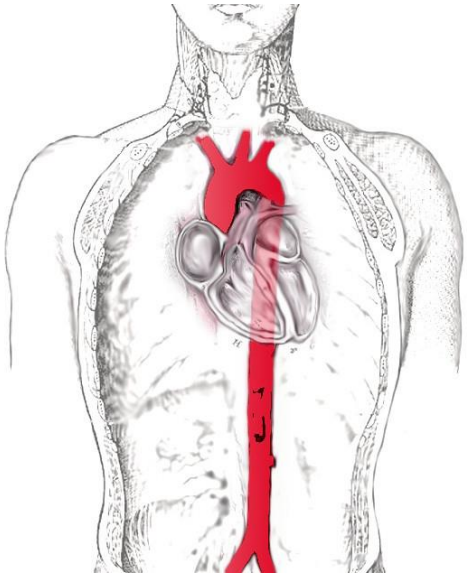

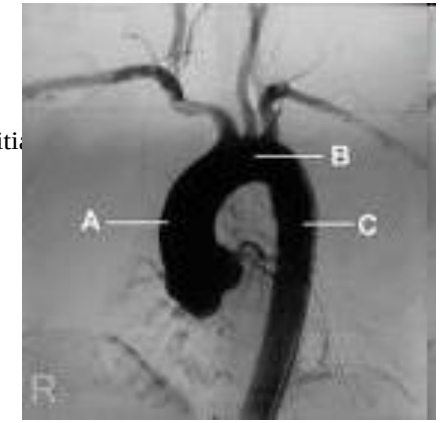

avril@emse.fr

Basics of aortic mechanics

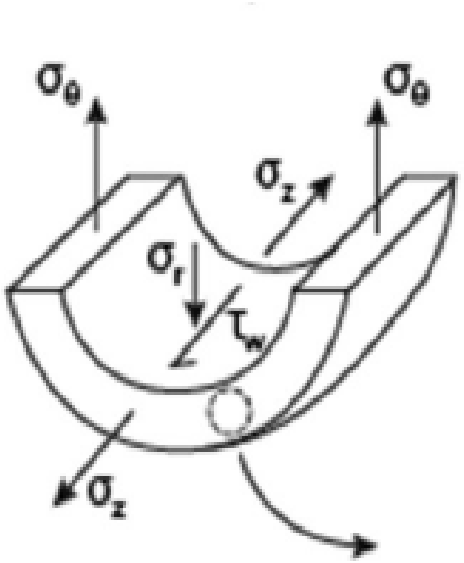

$$\tau_w = \frac{4\mu Q}{\pi a^3}, \qquad \sigma_\theta = \frac{P a}{h}$$

$$\sigma_z = \frac{f_z}{\pi\left(b^2 - a^2\right)} = \frac{f_z}{\pi h\left(2a - h\right)}$$

Humphrey JD (2002) *Cardiovascular Solid Mechanics: Cells, Tissues, and Organs*, Springer-Verlag, NY

Functional biomechanical behavior

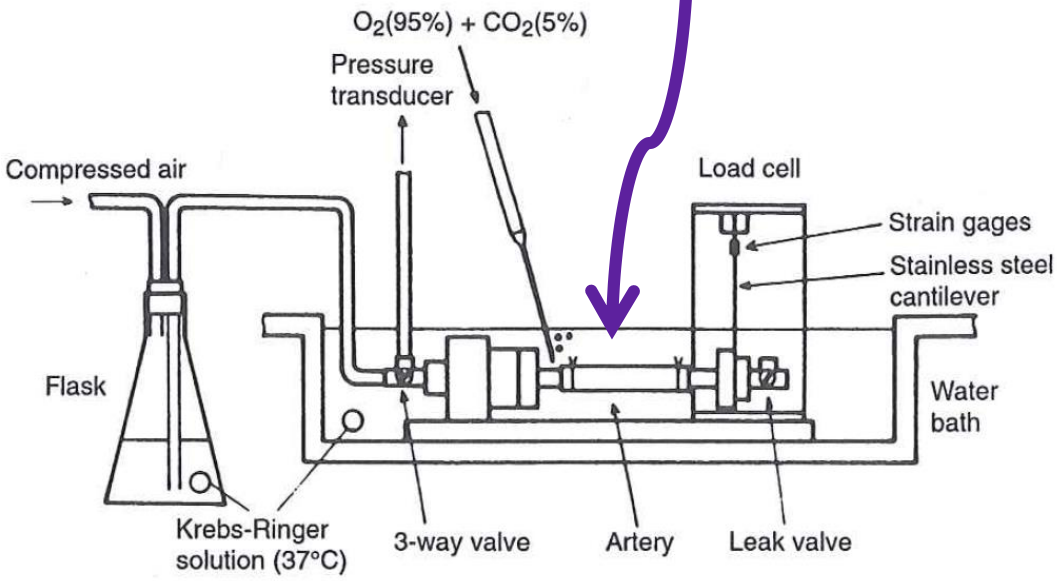

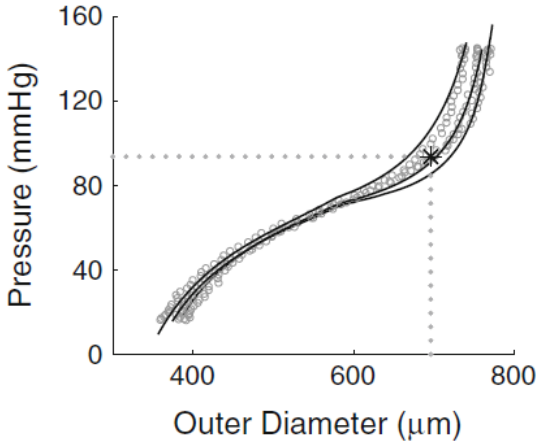

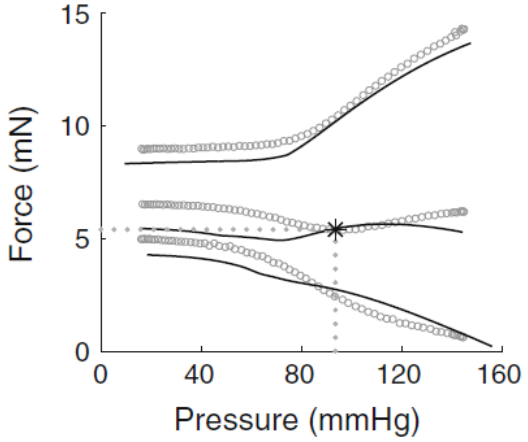

Material characterization and constitutive modeling

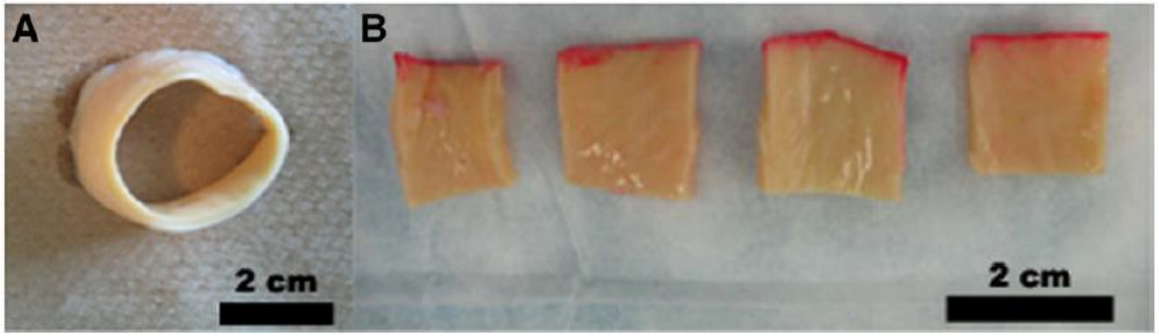

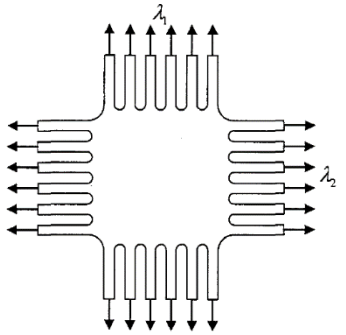

$$W = C_{10}\left(\overline{I}_1 - 3\right) + \frac{1}{D}\left(\frac{J^2-1}{2} - \ln J\right)$$
$$+ \frac{k_1}{2k_2}\sum_{\alpha=1}^{N}\left\{\exp\left[k_2\left\langle \overline{E}_\alpha\right\rangle^2\right] - 1\right\}$$

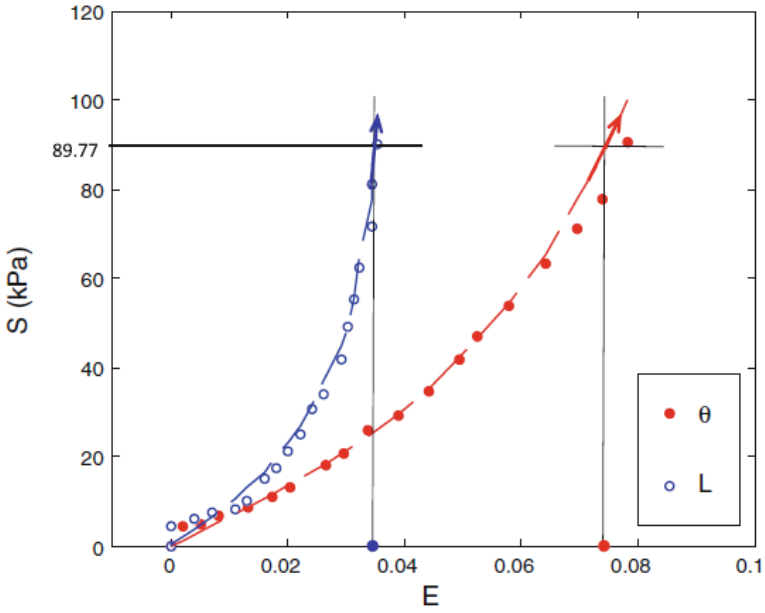

avril@emse.fr

Prediction of risk of rupture and dissection

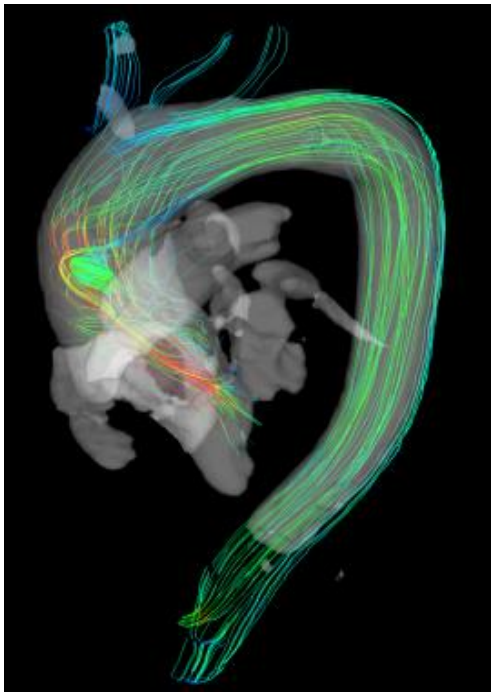

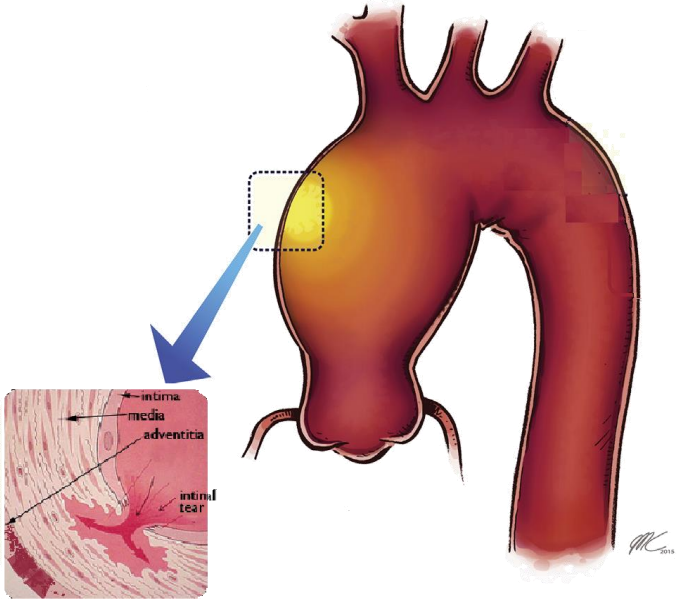

dissection

avril@emse.fr

MEASUREMENT OF THE RESPONSE USING DIGITAL IMAGE CORRELATION

classical

panoramic

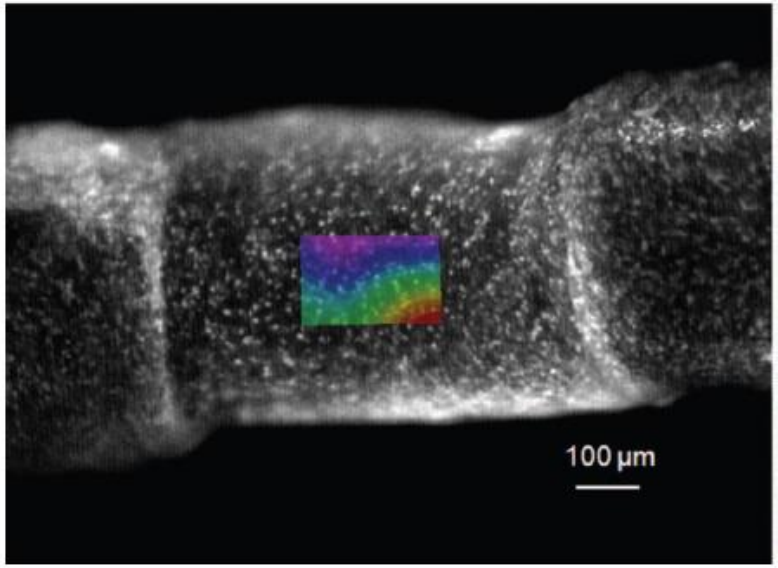

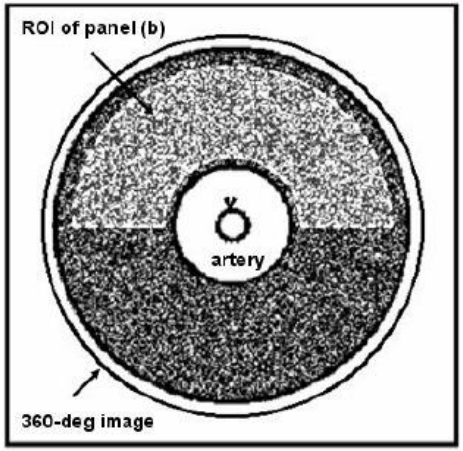

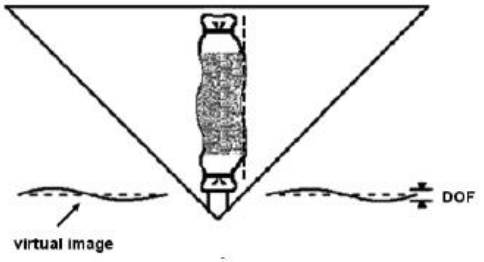

Badel et al. CMBBE, **15**, p 37-48, 2012.

Genovese. Optics Lasers Eng, **47**, p 995-1008, 2009.

Collection of the samples

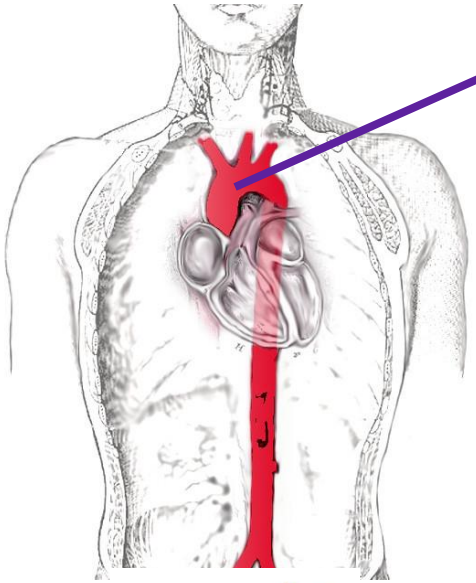

CHU Saint-Étienne

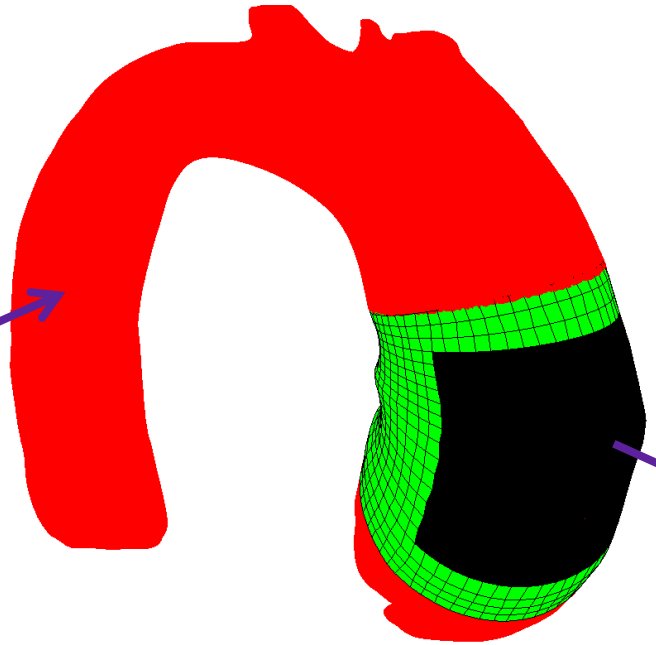

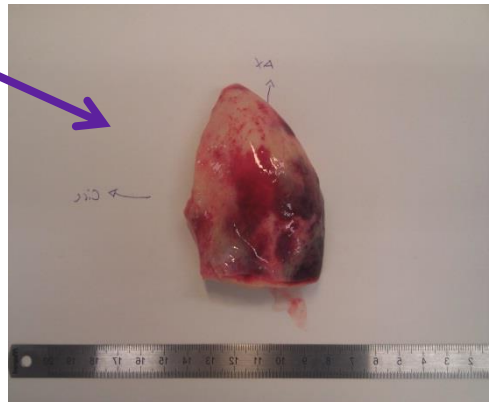

avril@emse.fr

MINES Saint-Étienne

Preparation

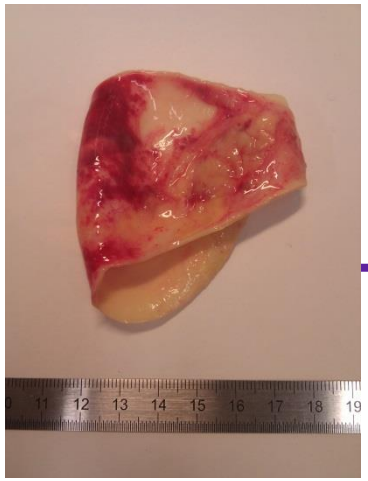

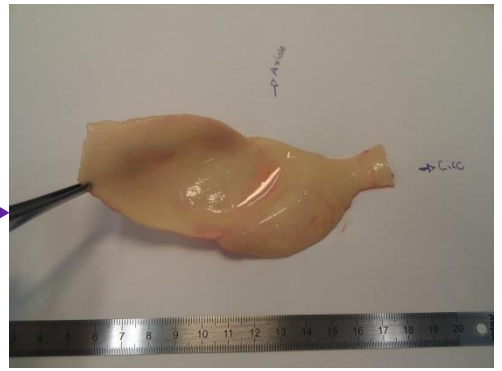

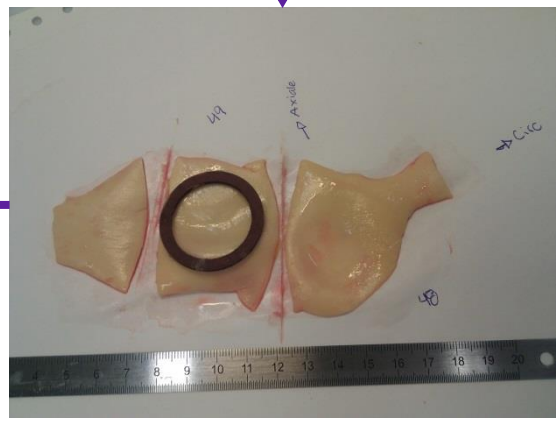

avril@emse.fr

Bulge inflation test

Romo et al. Journal of Biomechanics -2014.

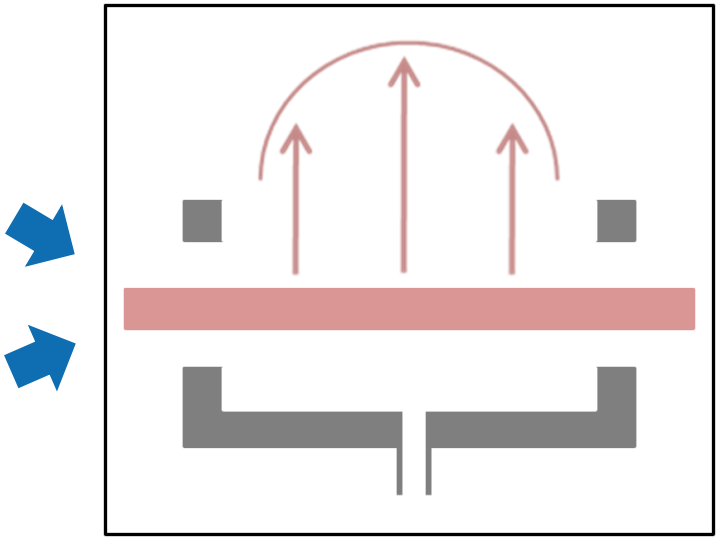

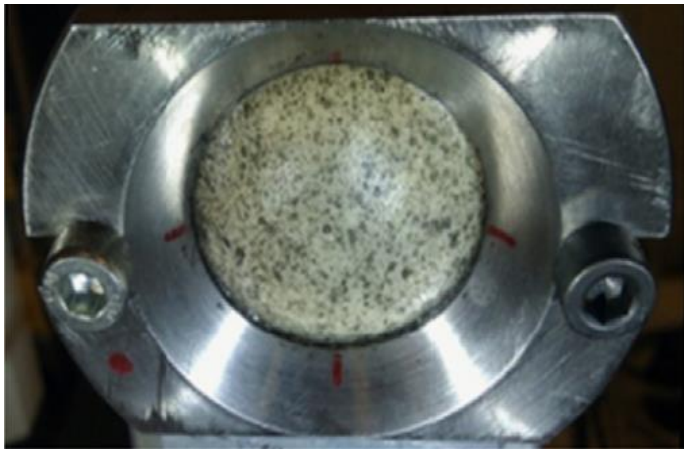

avril@emse.fr

Full-field measurements using sDIC

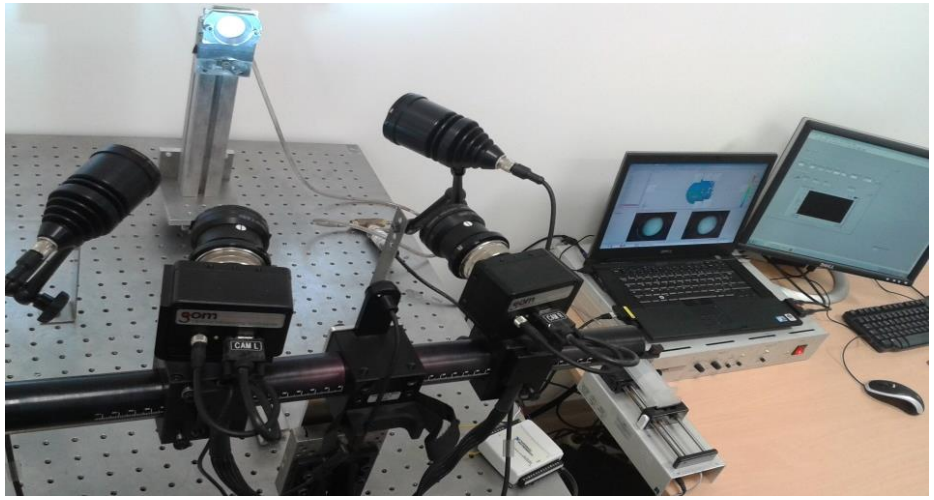

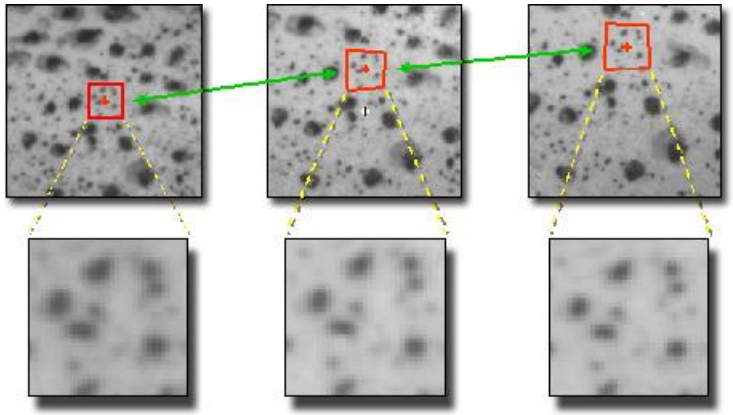

Undeformed

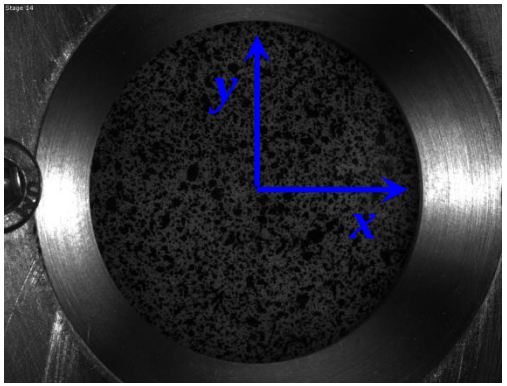

Deformed

avril@emse.fr

Rupture profiles

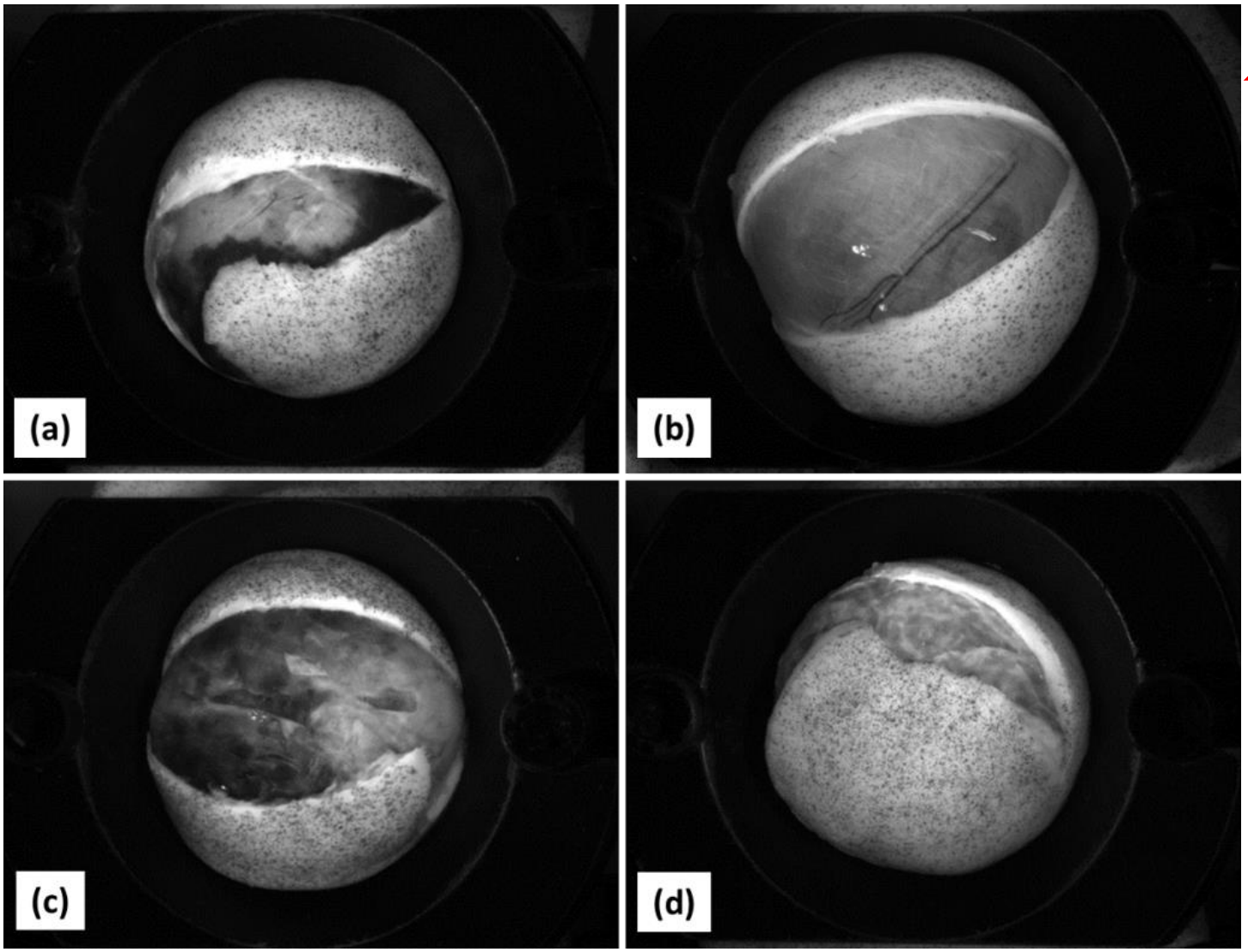

Blood flow

50% of aortas ruptured with an angle θ equal to 90 °

Identification of local material properties

THE UNIVERSITY OF IOWA

The WHITAKER Foundation

Davis et al. BMMB – 2015.
Davis et al. JMBBM – 2016
Zhao et al. Acta Biomaterialia - 2016

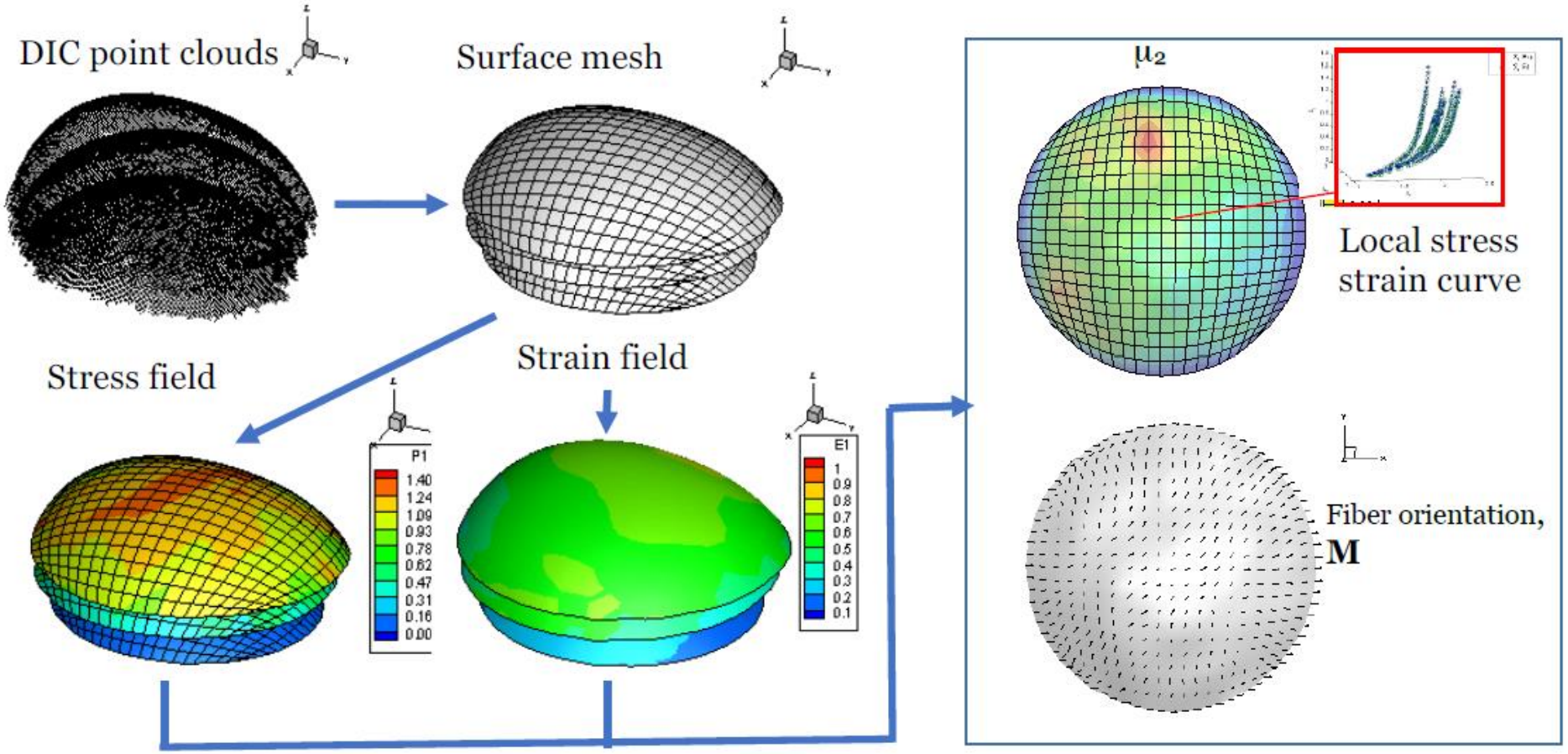

avril@emse.fr

MINES Saint-Étienne

Rupture risk estimation

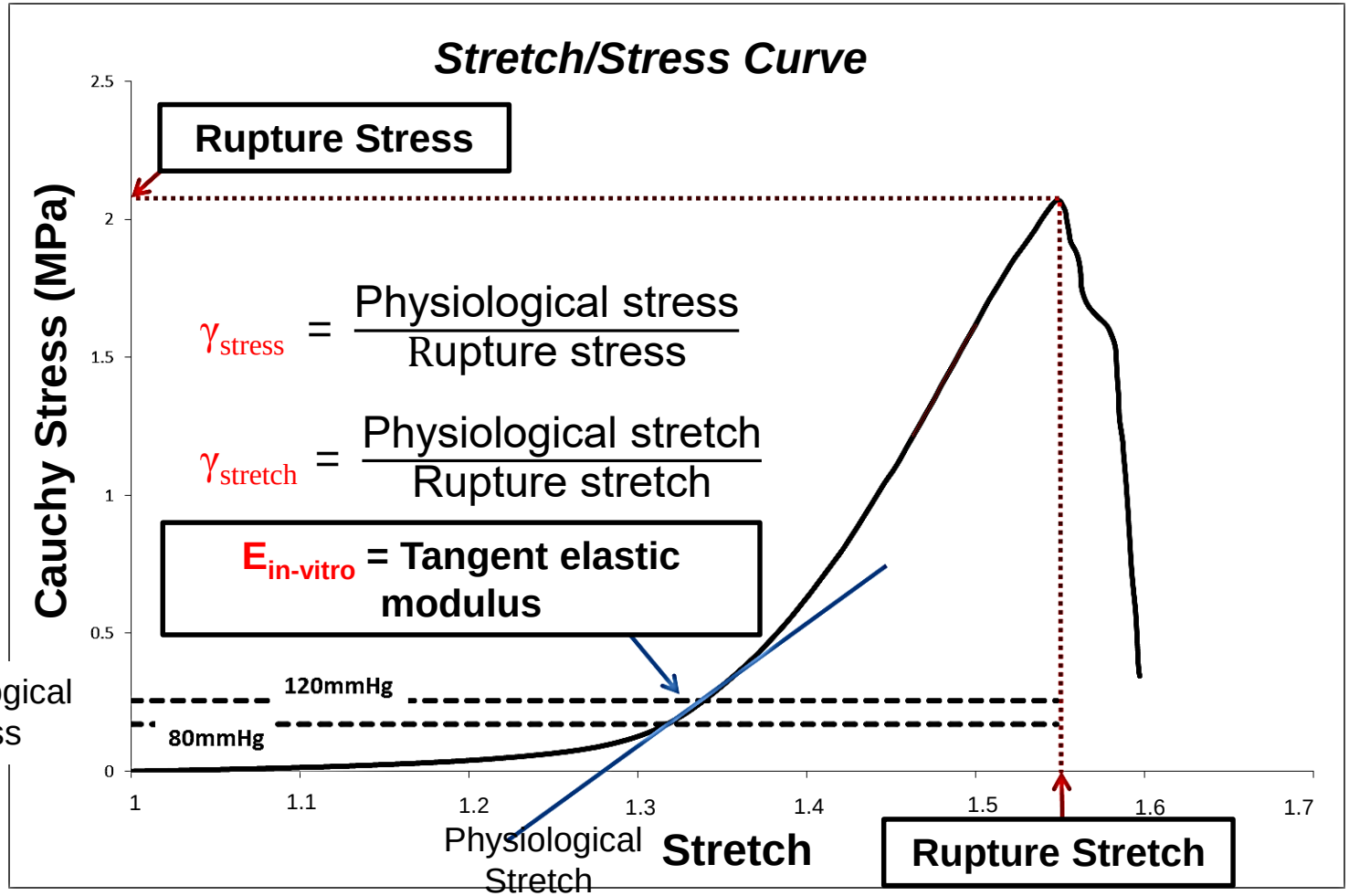

avril@emse.fr

Correlation between the stretch-based rupture risk and the tangent elastic modulus

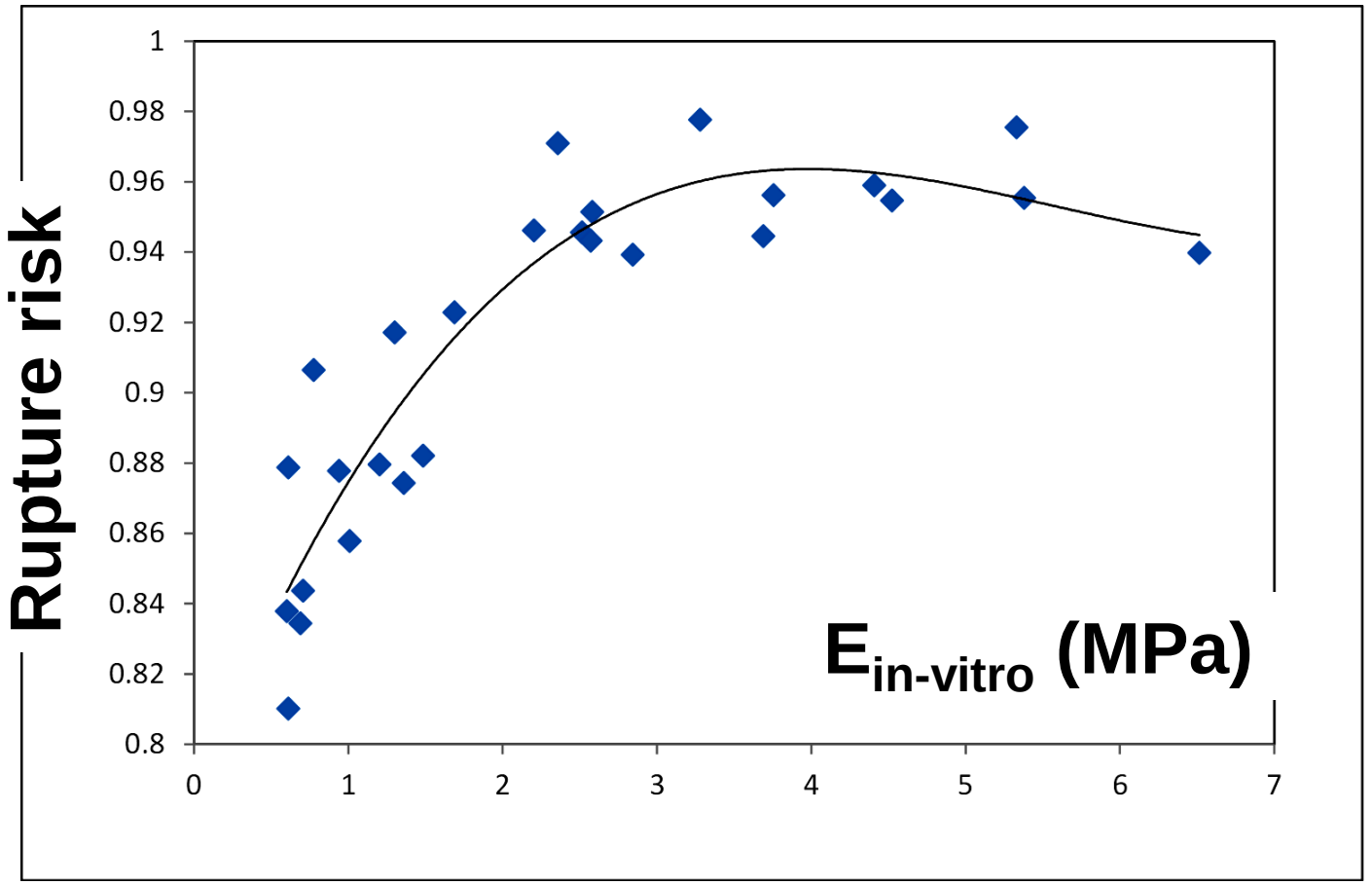

Duprey A, et al. Biaxial rupture properties of ascending thoracic aortic aneurysms. ***Acta Biomaterialia 2016.***

Understanding aneurysm growth using mechanobiology and photomechanics

avril@emse.fr

Altered mechanics induce biological responses, including gene expression, protein activation and cell phenotype

avril@emse.fr

APPROACH

1. Experiments
2. Material model
3. Inverse method

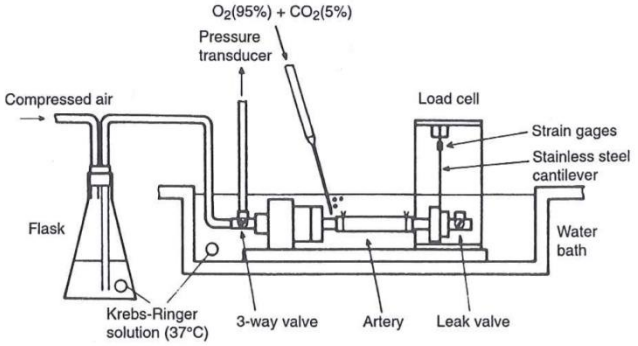

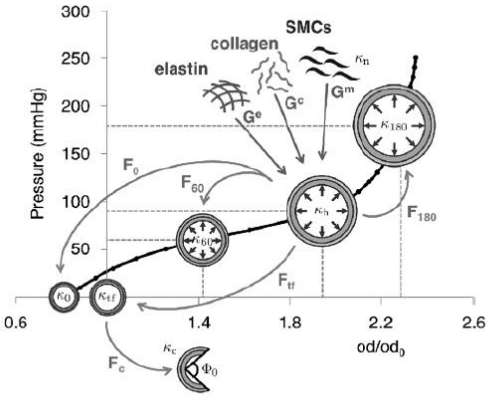

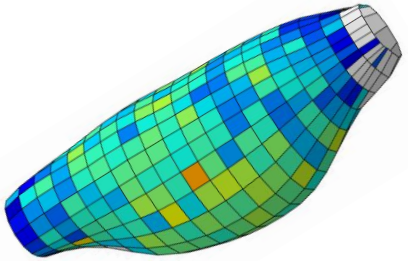

avril@emse.fr

Study Design

Control

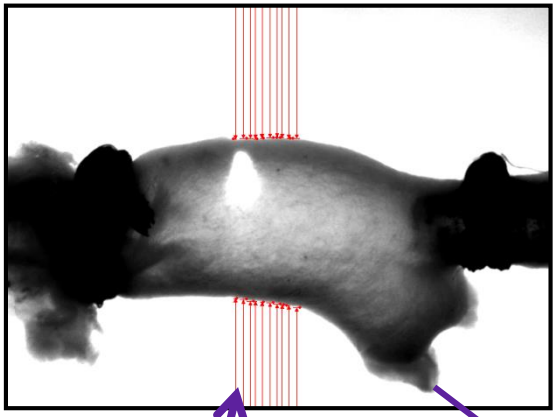

Fibulin 4 SMC KO

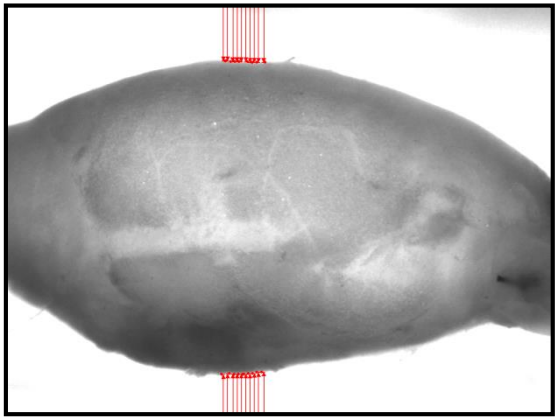

Fibrillin 1 *mgR/mgR*

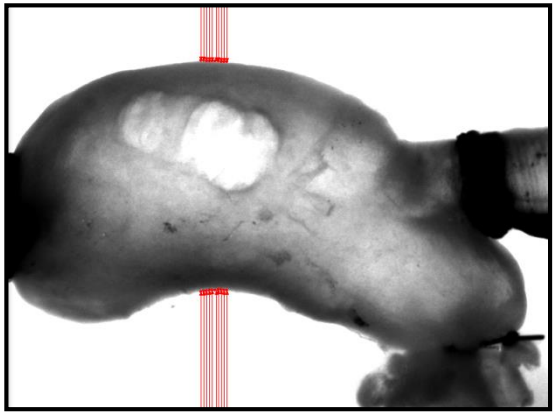

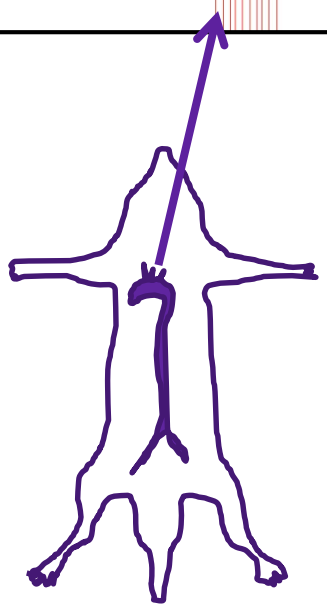

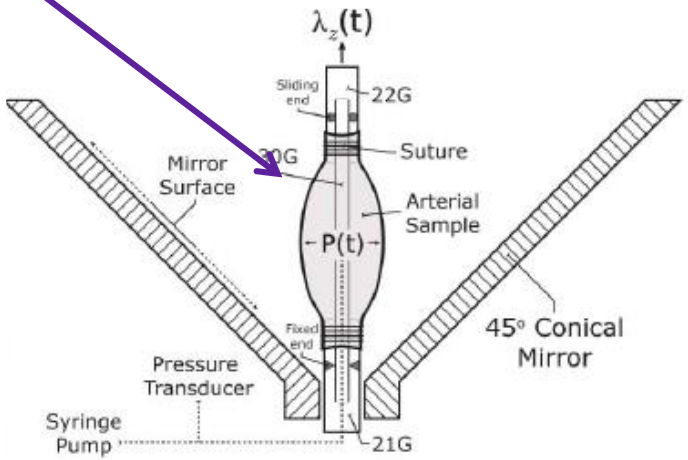

avril@emse.fr

The pDIC technique

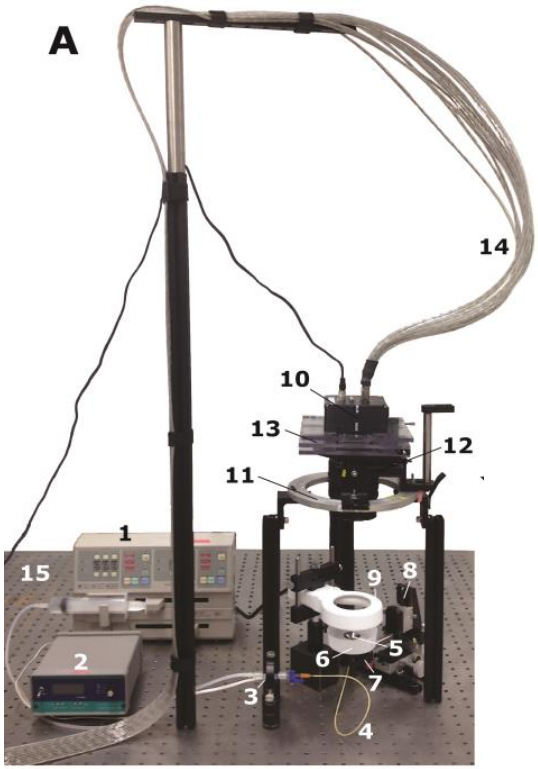

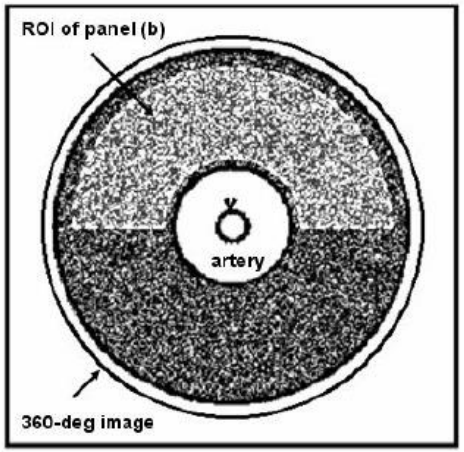

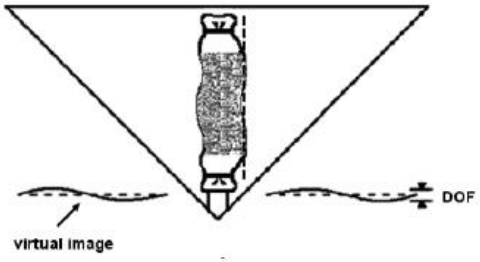

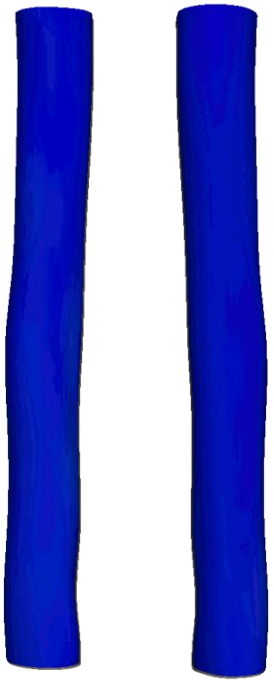

Posterior Anterior

avril@emse.fr

MINES Saint-Étienne

pDIC measurements

Fibulin 4 SMC KO

ventral *dorsal* *inflation*

6852

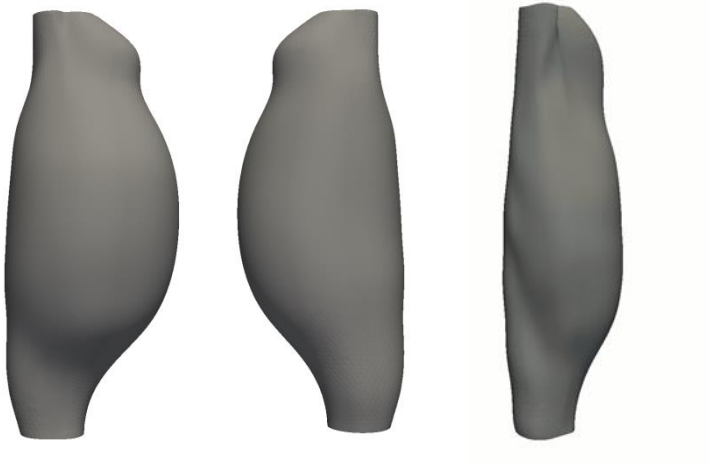

Fibrillin 1 *mgR/mgR*

ventral *dorsal* *inflation*

CS38

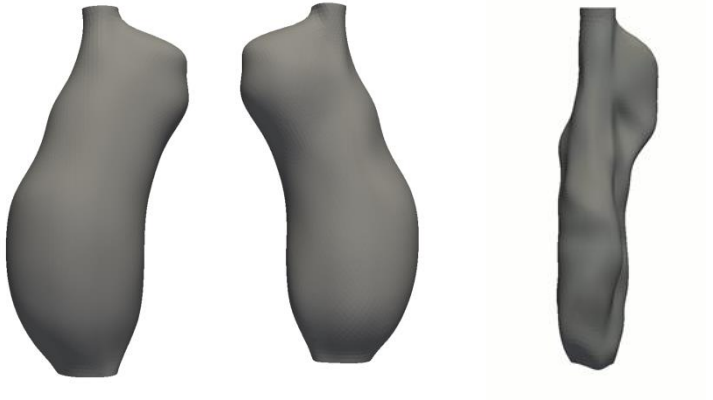

avril@emse.fr

OCT-DVC applied to arterial mechanics

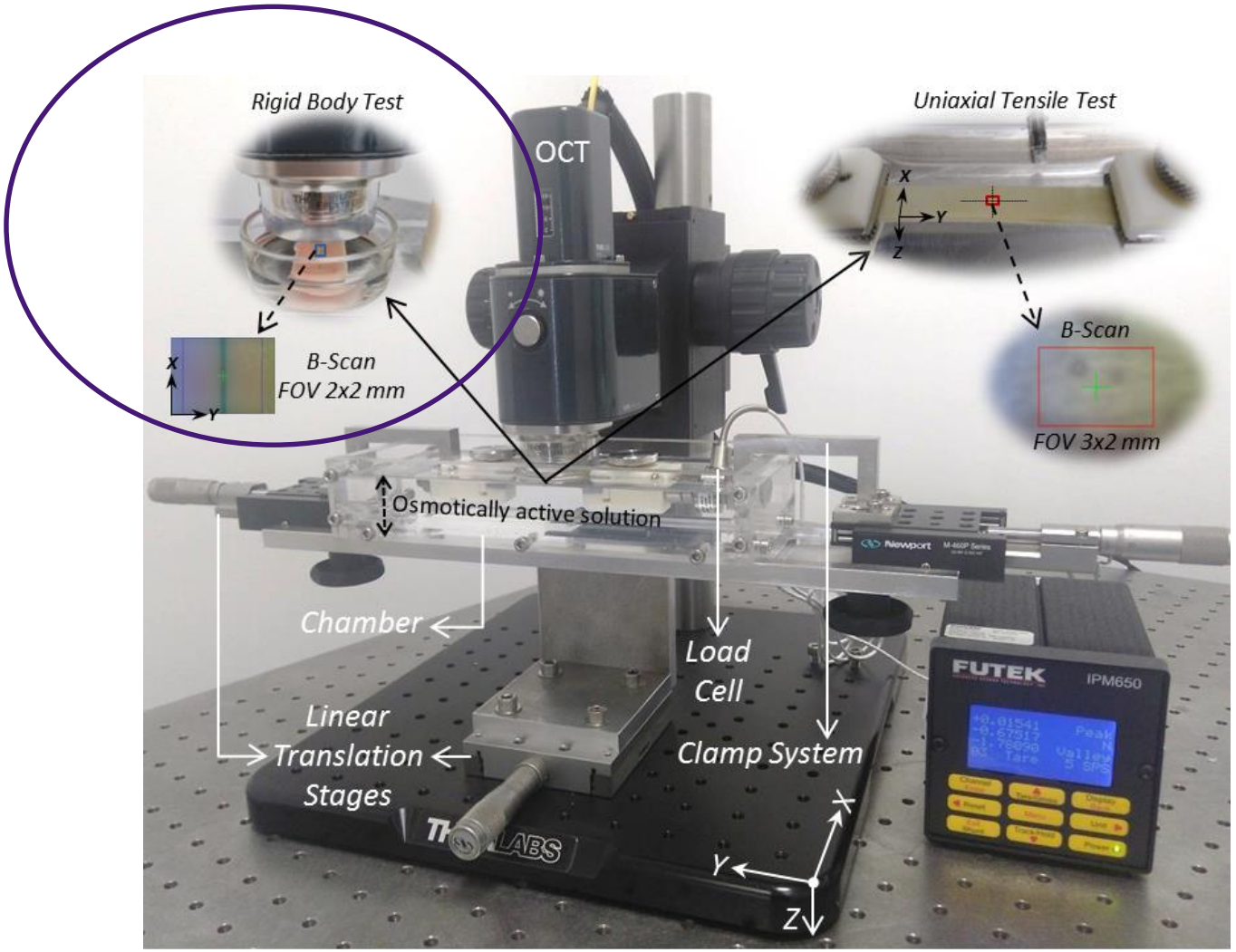

avril@emse.fr

MINES Saint-Étienne

Measurement of bulk deformation fields by Digital Volume Correlation on OCT images

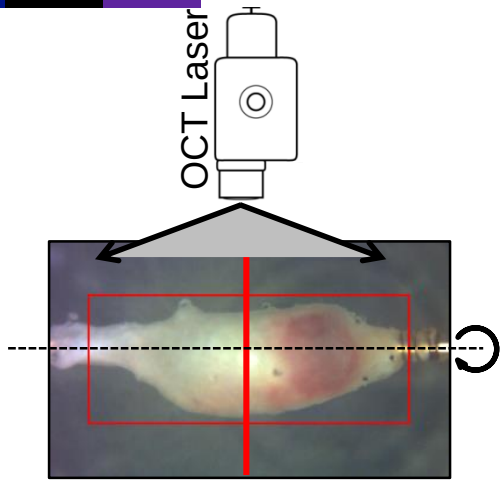

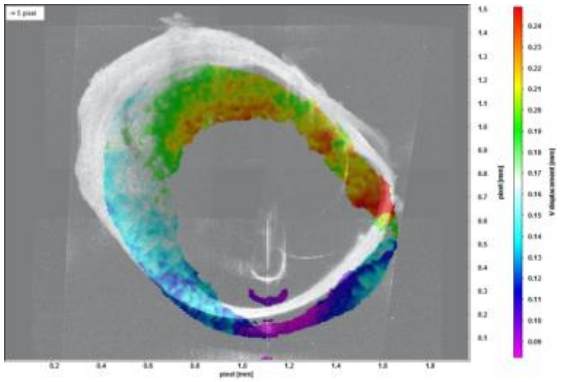

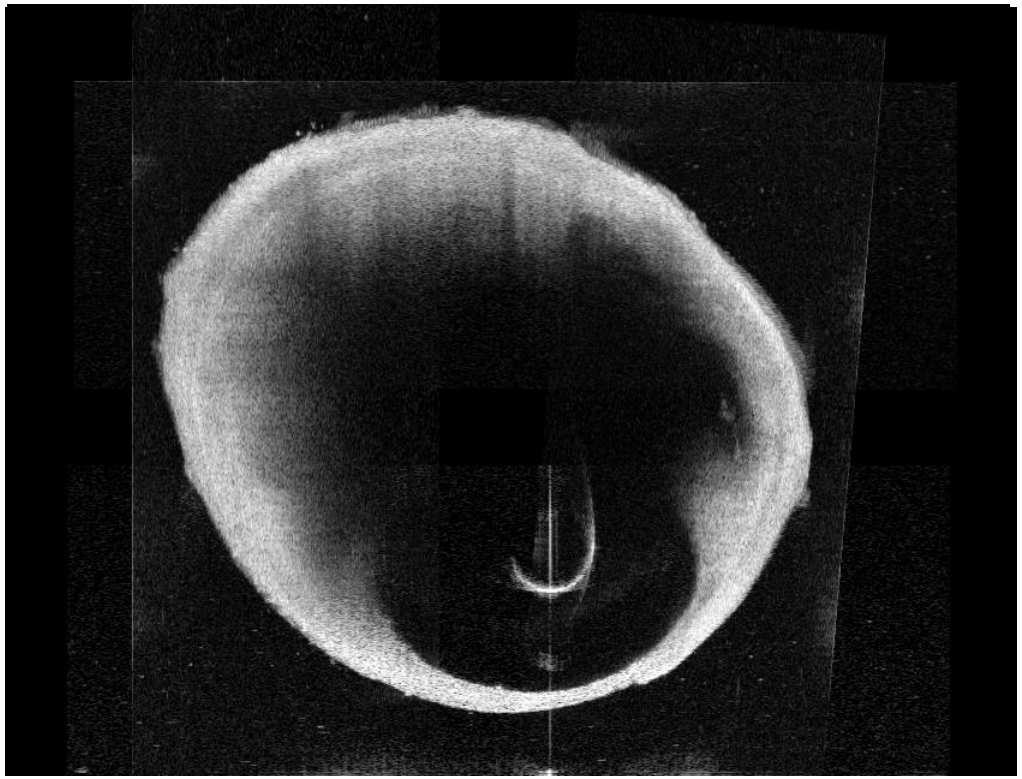

avril@emse.fr

Image Processing Methodology – Inflation Test

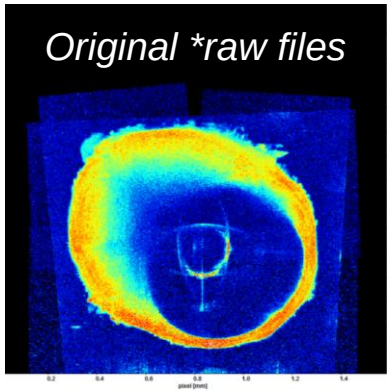

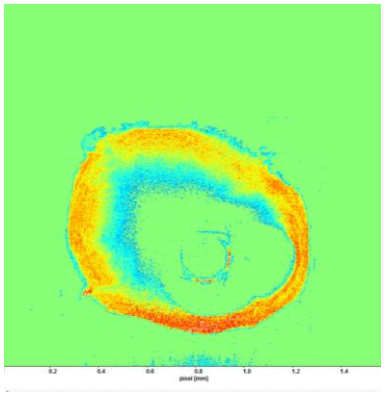

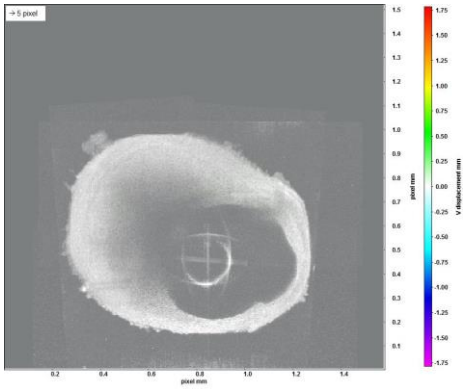

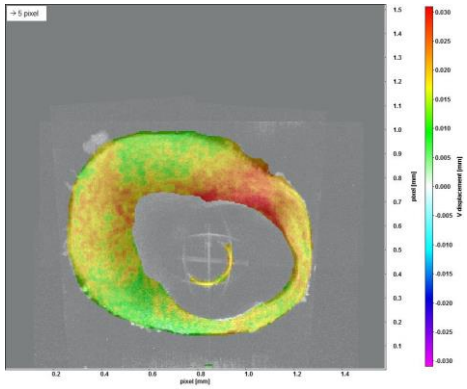

Title: REF
Width: 667 pixels
Height: 640 pixels
Depth: 100 pixels
Voxel size: 1x1x1 pixel^3 (2.38um)

Original Image Parameters

Pressures: 20, 40, 60, 80, 100, 120, 140
Lambda (λ) 1 – 2 – 3

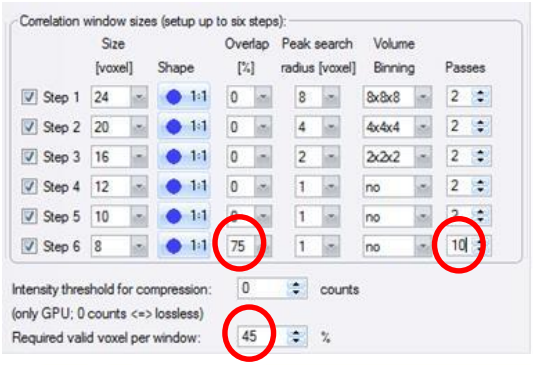

- ***Algorithmic Mask – Threshhold: 48***
- ***Correlation window size [voxel]: 24 (8x8x8)***
- ***Overlap : 75%***
- ***Passes : 10***
- ***Required valid voxel per window: 44%***

avril@emse.fr

MINES Saint-Étienne

APPROACH

1. Experiments
2. Material model
3. Inverse method

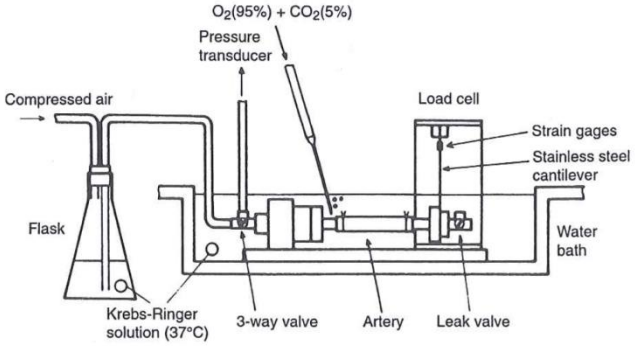

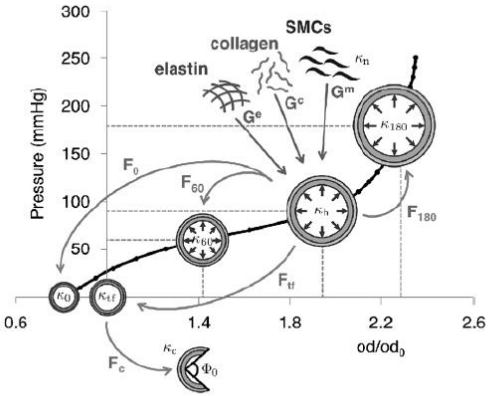

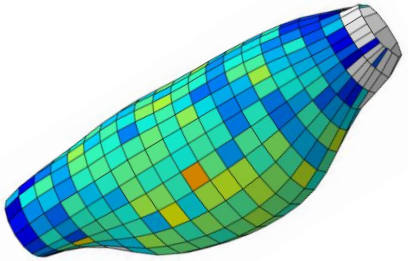

avril@emse.fr

CONSTITUTIVE MODEL

Strain energy functions:

$$W = \phi^{e} W^{e}(\mathbf{F}^{e}) + \phi^{m} W^{m}(\lambda^{m}) + \sum_{j=1}^{4} \phi^{c_j} W^{c_j}(\lambda^{c_j})$$

$$W^{e}(\mathbf{F}^{e}) = \frac{c^{e}}{2}\left[\mathrm{tr}\left((\mathbf{F}^{e})^{T}\mathbf{F}^{e}\right) - 3\right]$$

$$W^{m}(\lambda^{m}) = \frac{c_2^{m}}{4c_3^{m}}\left[e^{c_3^{m}\left((\lambda^{m})^2-1\right)^2} - 1\right]$$

$$W^{c}(\lambda^{c_j}) = \frac{c_2^{c}}{4c_3^{c}}\left[e^{c_3^{c}\left((\lambda^{c_j})^2-1\right)^2} - 1\right]$$

Bellini, et al., Ann. Biomed. Eng., **42**(3), pp. 488–502, 2014

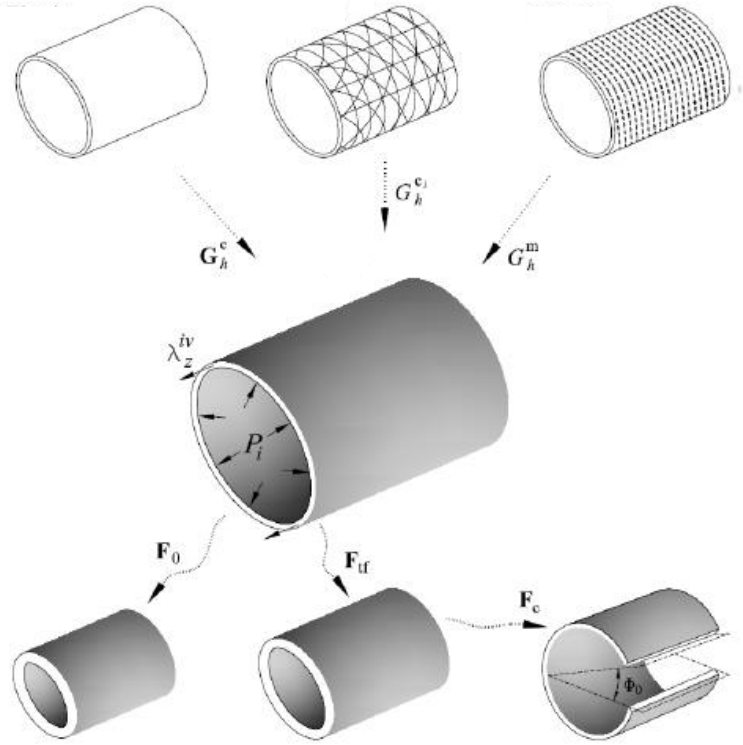

avril@emse.fr

PARAMETERS TO BE IDENTIFIED

$$W = \phi^{e} W^{e}(\mathbf{F}^{e}) + \phi^{m} W^{m}(\lambda^{m}) + \sum_{j=1}^{4} \phi^{c_j} W^{c_j}(\lambda^{c_j})$$

$$W^{e}(\mathbf{F}^{e}) = \frac{c^{e}}{2}\left[\mathrm{tr}\left((\mathbf{F}^{e})^{T}\mathbf{F}^{e}\right) - 3\right]$$

$$W^{m}(\lambda^{m}) = \frac{c_2^{m}}{4c_3^{m}}\left[e^{c_3^{m}(\lambda^{m})^2-1)^2} - 1\right]$$

$$W^{c}(\lambda^{c_j}) = \frac{c_2^{c}}{4c_3^{c}}\left[e^{c_3^{c}(\lambda^{c_j})^2-1)^2} - 1\right]$$

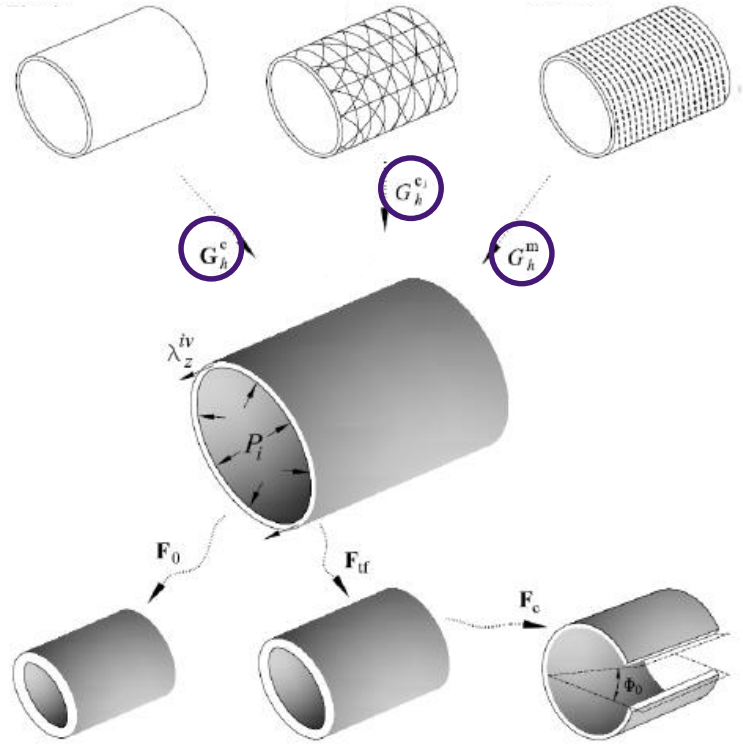

avril@emse.fr

APPROACH

1. Experiments
2. Material model
3. Inverse method

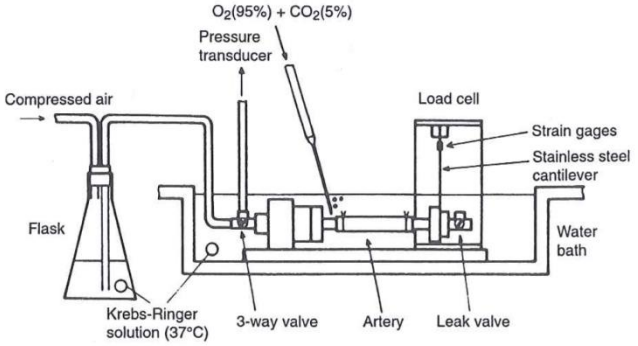

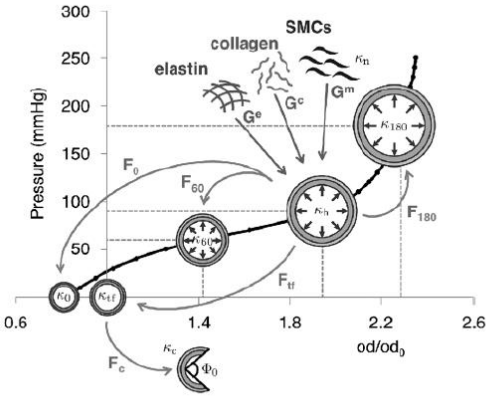

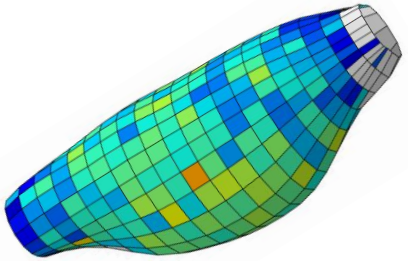

avril@emse.fr

Inverse approach – traditional approach

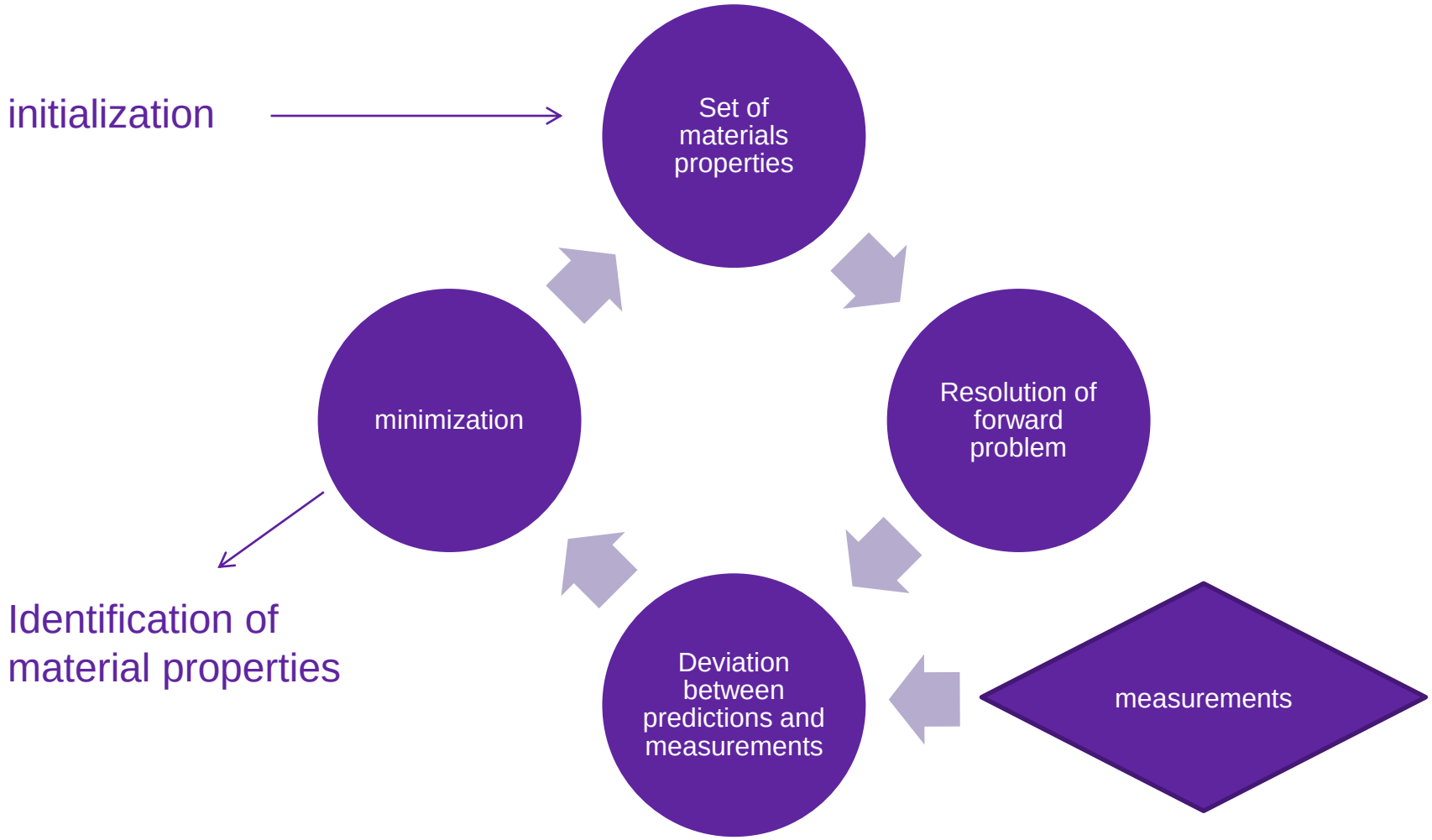

Inverse approach – FEMU approach

initialization ⟶

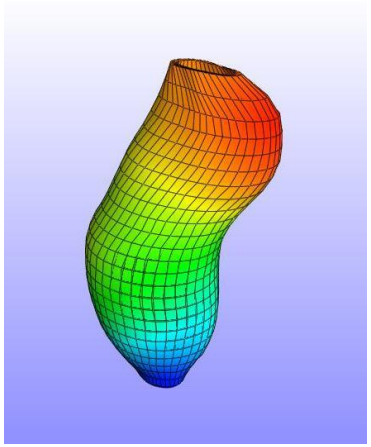

$$J(\mu) = \|T(u) - T(u^{exp})\|^2 + \frac{\alpha}{2} B(\mu)$$

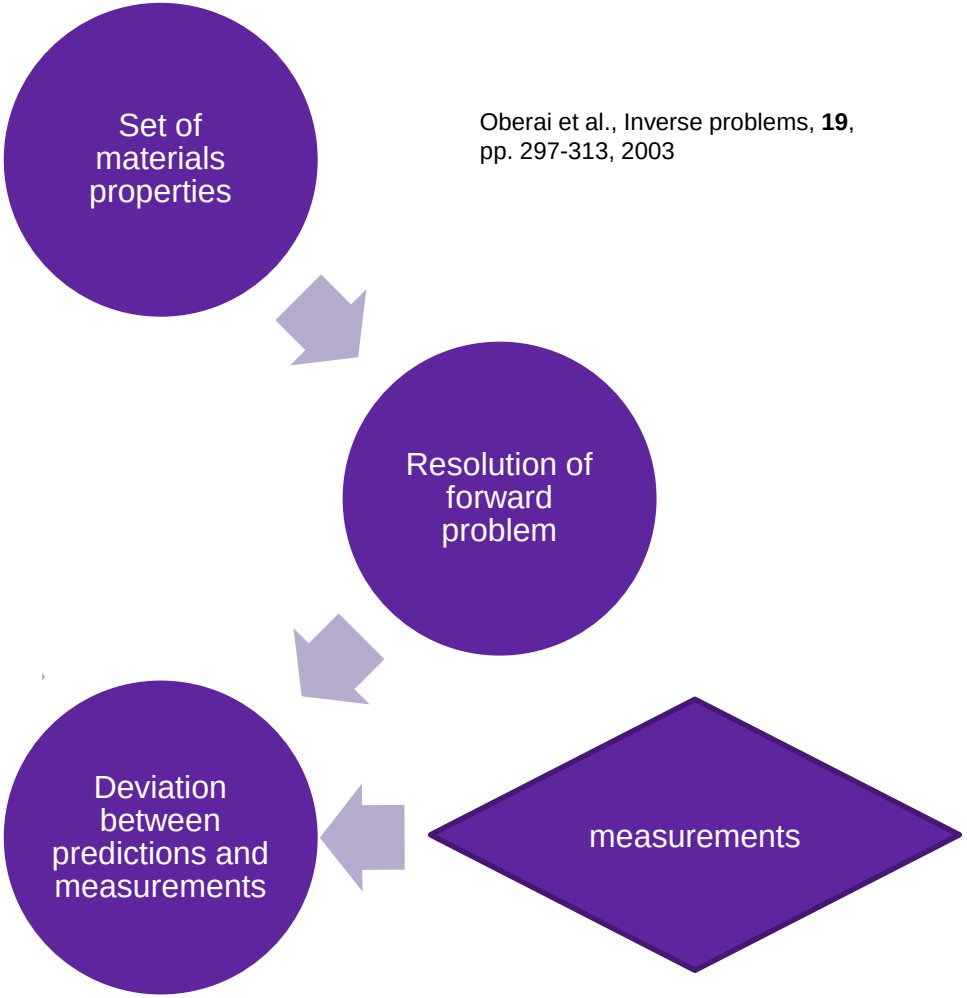

Oberai et al., Inverse problems, **19**, pp. 297-313, 2003

Inverse approach – FEMU approach

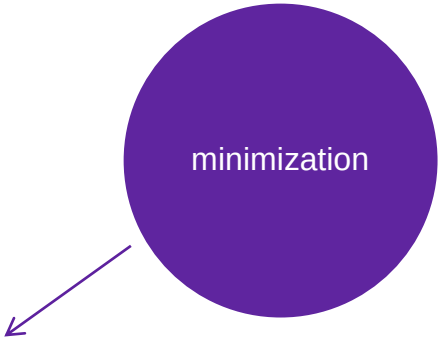

Identification of material properties

1. Use a gradient based method (steepest descent or BFGS)
2. Need to derive the gradient of J with respect to μ at each iteration. With the adjoint method, this requires the resolution of 2 forward problems
3. Very unstable with hyperelastic models: **many risks that the forward problems have a poor convergence**

Alternative inverse approach: the virtual fields method

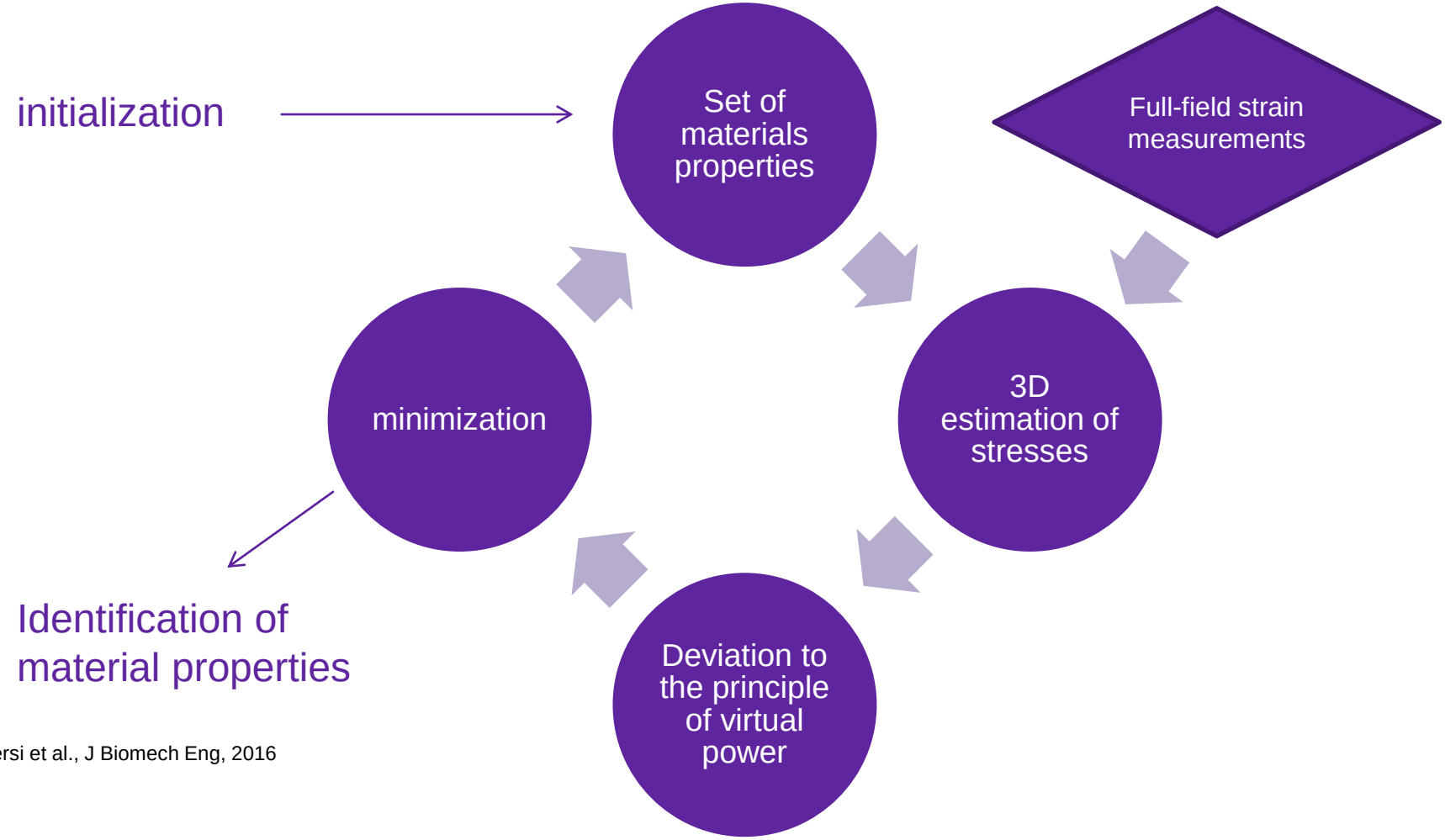

Bersi et al., J Biomech Eng, 2016

Full-field stress reconstruction

initialization

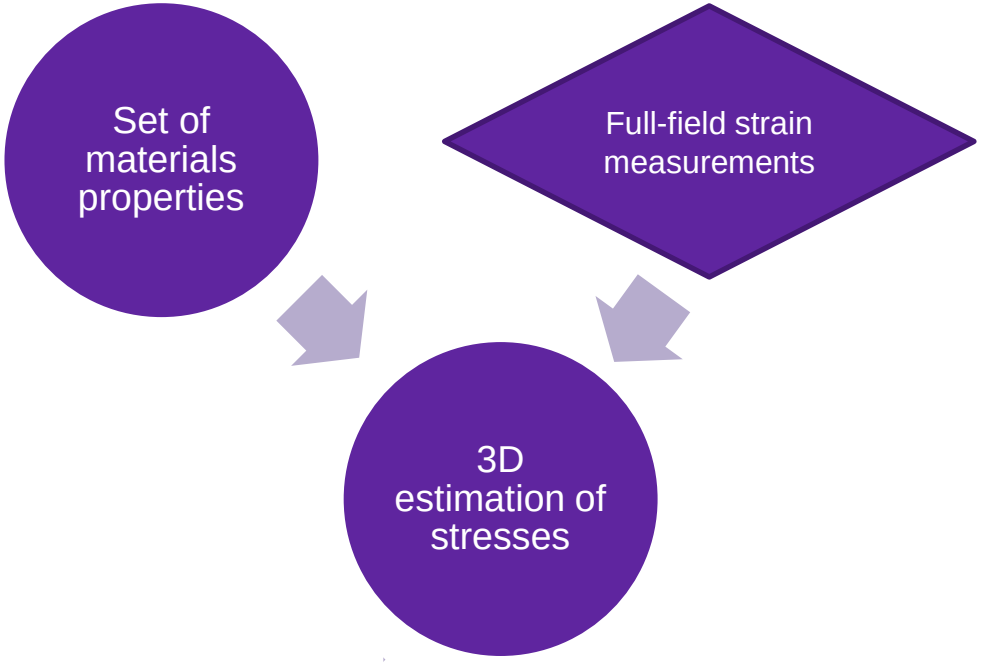

$$W = \phi^{e} W^{e}(\mathbf{F}^{e}) + \phi^{m} W^{m}(\lambda^{m}) + \sum_{j=1}^{4} \phi^{c_j} W^{c_j}(\lambda^{c_j})$$

$$W^{e}(\mathbf{F}^{e}) = \frac{c^{e}}{2}\left[\mathrm{tr}\left((\mathbf{F}^{e})^{T}\mathbf{F}^{e}\right) - 3\right]$$

$$W^{m}(\lambda^{m}) = \frac{c_2^{m}}{4c_3^{m}}\left[e^{c_3^{m}\left((\lambda^{m})^2-1\right)^2} - 1\right]$$

$$W^{c}(\lambda^{c_j}) = \frac{c_2^{c}}{4c_3^{c}}\left[e^{c_3^{c}\left((\lambda^{c_j})^2-1\right)^2} - 1\right]$$

Simple application of the constitutive model for each element

avril@emse.fr

Minimization of the equilibrium gap using the principle of virtual power

minimization

$$J = \sum_{p} \sum_{\lambda} \left(\underbrace{-\int_{\omega(t)} \underline{\underline{\sigma}} : \left(\underline{\nabla} \otimes \underline{\xi}^* \right) d\omega}_{P^*_{int}} + \underbrace{\oint_{\partial\omega(t)} \underline{T} : \underline{\xi}^* \, ds}_{P^*_{ext}} \right)^2$$

Bersi et al., J Biomech Eng, 2016

Resolution:

$$\min_{c_3^1, c_3^{2,3}, c_3^4, \alpha, \beta} \left[\min_{c^e, c_2^1, c_2^{2,3}, c_2^4} \left[\frac{J(u)}{A} + \frac{J(v)}{B} \right] \right]$$

Linear least-squares

Genetic algorithm

avril@emse.fr

MINES Saint-Étienne

Derivation of stress tensor using layer specific constitutive behavior

3D estimation of strains

3D estimation of stress

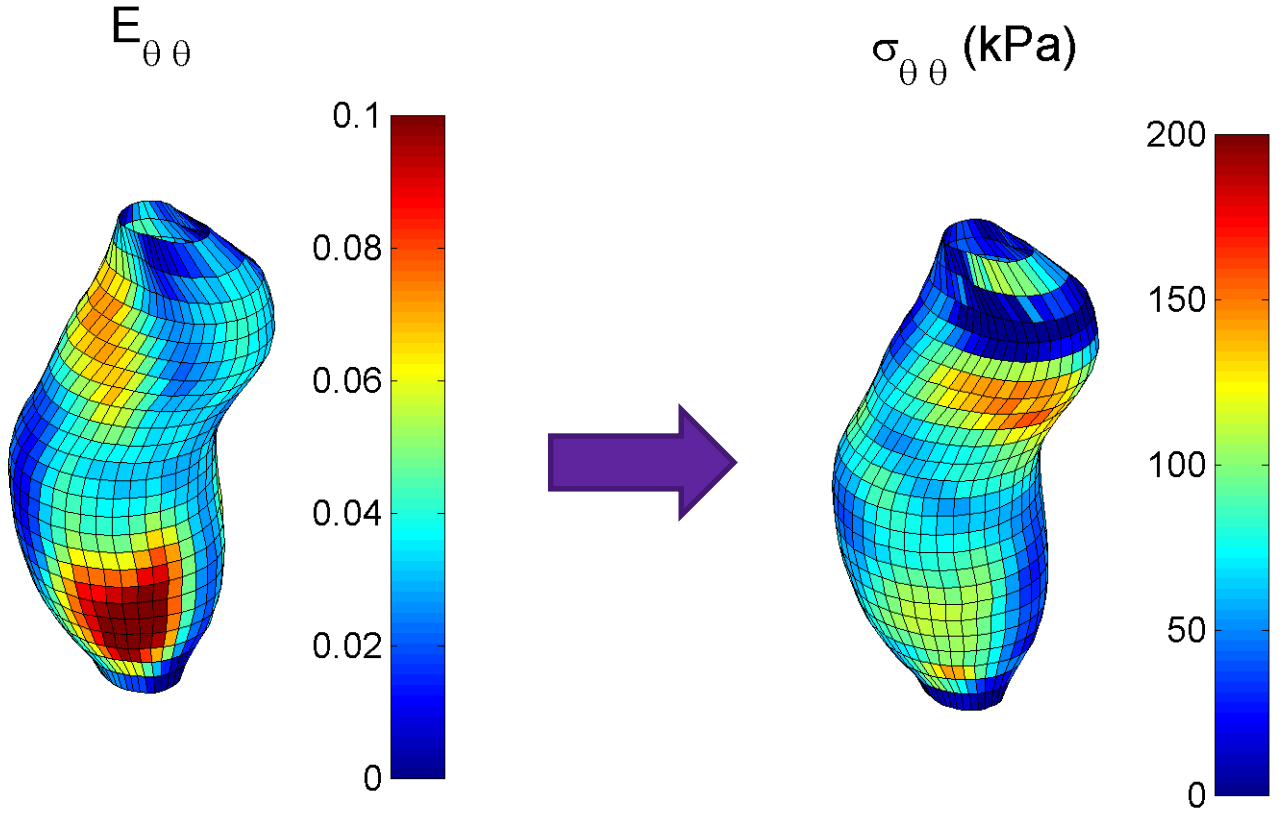

avril@emse.fr

Virtual power 1

1. A local virtual radial “bulge”: $\mathbf{u}(\mathbf{x}) = [f(\mathbf{x}-\mathbf{x}_0)/r^2]\,\mathbf{e}_r$

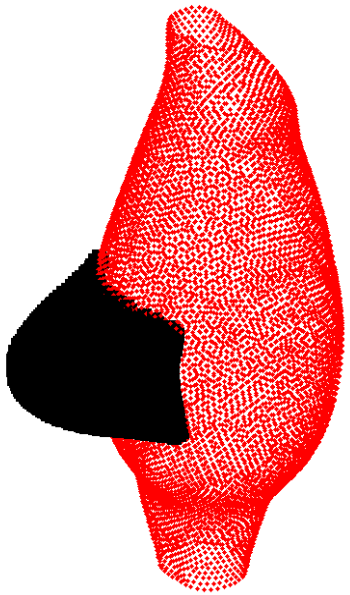

$$\underbrace{-\int_{\omega(t)} \underline{\underline{\sigma}} : \left(\underline{\nabla} \otimes \underline{\xi}^*\right) d\omega}_{P^*_{int}} + \underbrace{\oint_{\partial\omega(t)} \underline{T} \cdot \underline{\xi}^* \, ds}_{P^*_{ext}} = 0$$

After deriving virtual strains (infinitesimal) local internal virtual work is derived at every Gauss point and integrated across the volume

The virtual field is normalized such as the external virtual work equals P.

Virtual power 2

2. Local virtual axial extension: $\mathbf{v}(\mathbf{x}) = f(\mathbf{x}-\mathbf{x}_0)\,(z\,\mathbf{e}_z - x/2\,\mathbf{e}_x - y/2\,\mathbf{e}_y)$

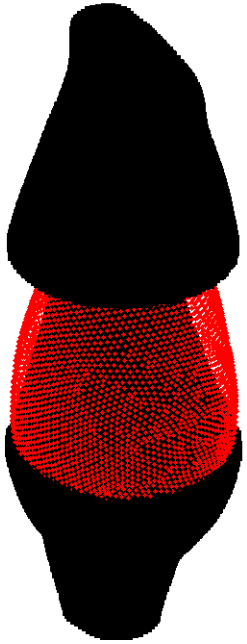

$$\underbrace{-\int_{\omega(t)} \underline{\underline{\sigma}} : \left(\underline{\underline{\nabla}} \otimes \underline{\xi}^*\right) d\omega}_{P^*_{int}} + \underbrace{\oint_{\partial\omega(t)} \underline{\underline{T}} : \underline{\xi}^*\, ds}_{P^*_{ext}} = 0$$

After deriving virtual strains (infinitesimal) local internal virtual work is derived at every Gauss point and integrated across the volume

The virtual field is normalized such as the external virtual work equals F.

Minimizing the equilibrium gap

minimization

$$J = \sum_{p} \sum_{\lambda} \left(\underbrace{-\int_{\omega(t)} \underline{\underline{\sigma}} : \left(\underline{\nabla} \otimes \underline{\xi}^* \right) d\omega}_{P^*_{int}} + \underbrace{\oint_{\partial\omega(t)} \underline{T} \cdot \underline{\xi}^* \, ds}_{P^*_{ext}} \right)^2$$

Bersi et al., J Biomech Eng, 2016

Resolution:

$$\min_{c_3^1, c_3^{2,3}, c_3^4, \alpha, \beta} \left[\underbrace{\min_{c^e, c_2^1, c_2^{2,3}, c_2^4} \left[\frac{J(u)}{A} + \frac{J(v)}{B} \right]}_{\text{Linear least-squares}} \right]$$

Genetic algorithm

avril@emse.fr

MINES Saint-Étienne

Similar to material fitting at every position

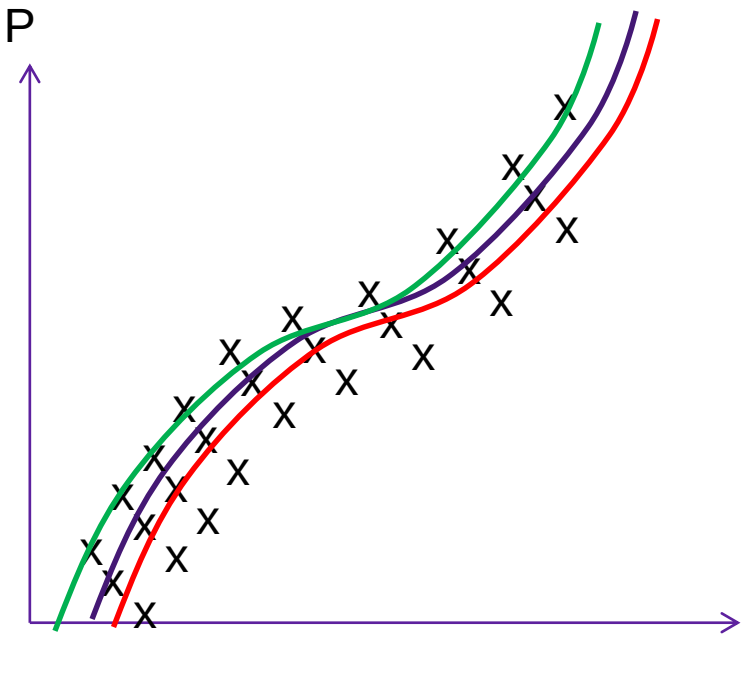

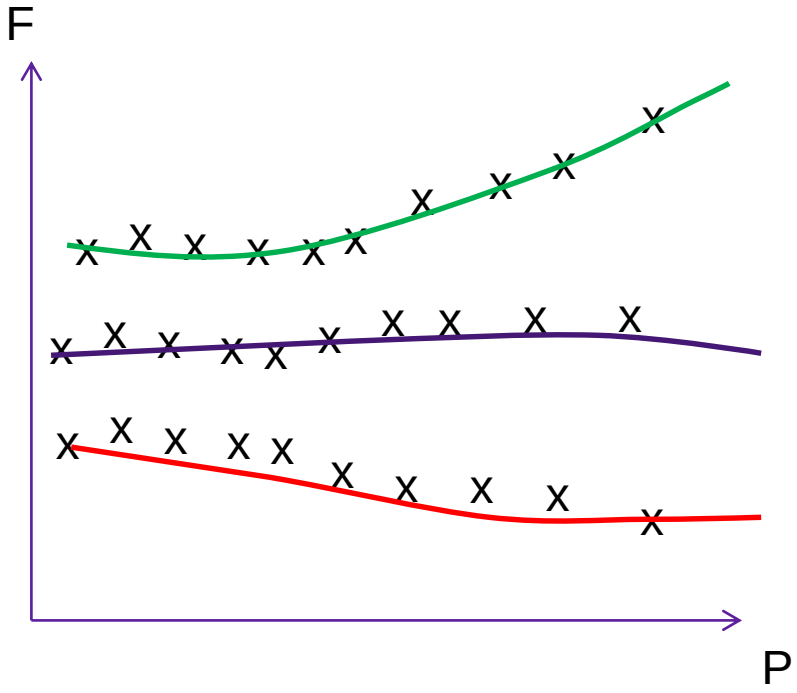

Crosses represent external virtual work for every pressure and axial stretch
Solid lines represent internal virtual work
The goodness of fit is evaluated with the R^2 value

Summary of the inverse approach

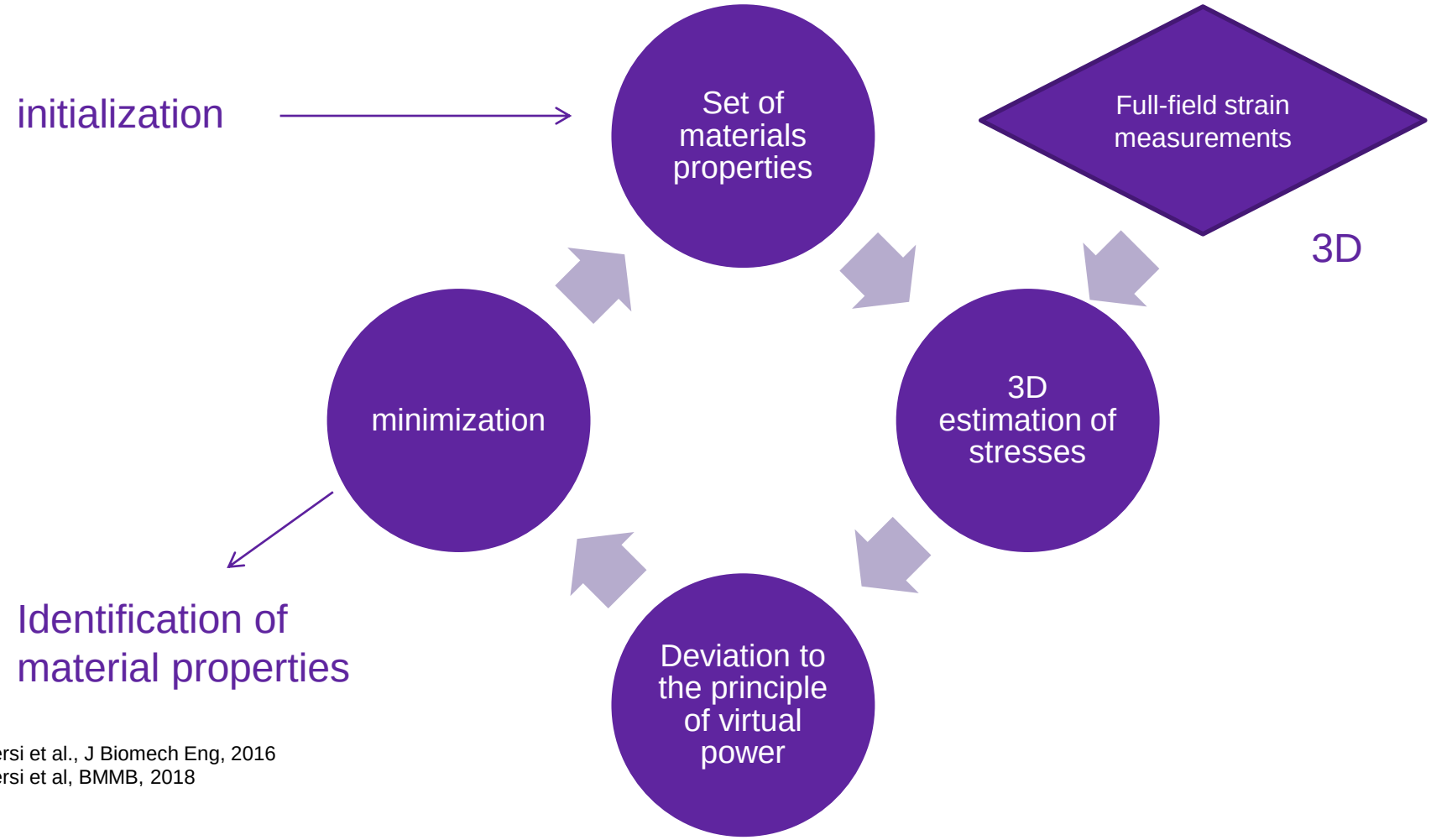

Bersi et al., J Biomech Eng, 2016
Bersi et al, BMMB, 2018

Results - Highlights

avril@emse.fr

DISSECTED ANEURYSMS

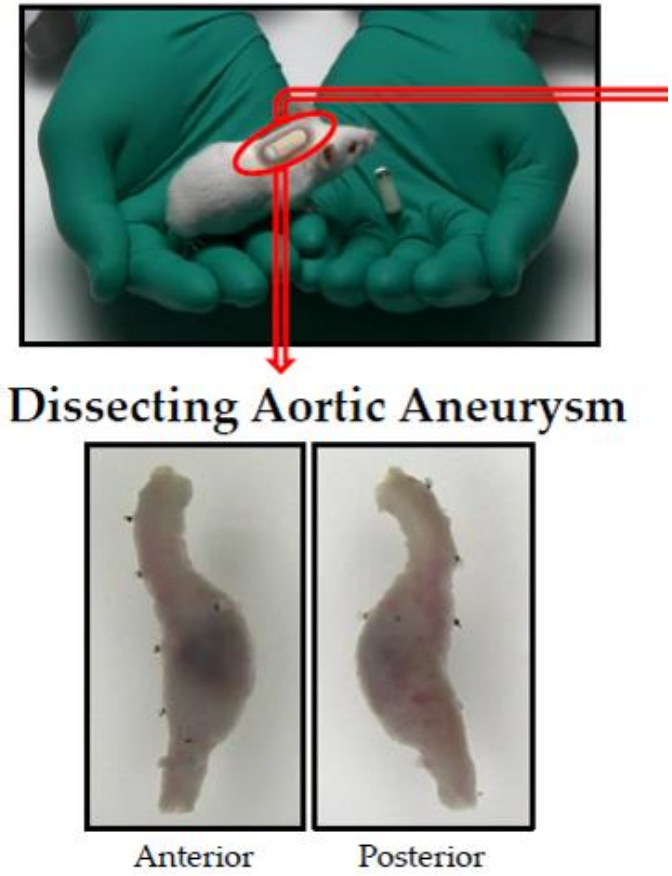

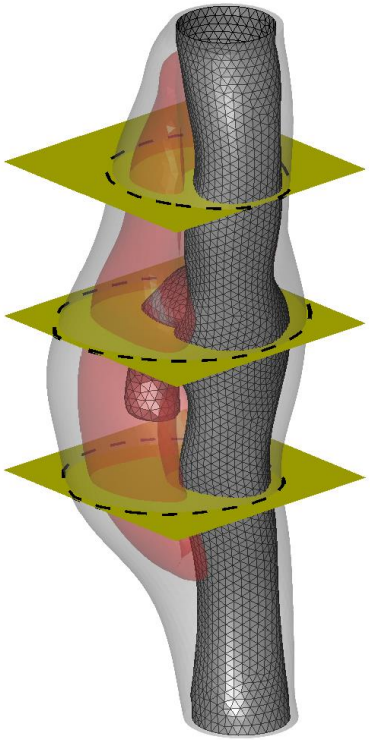

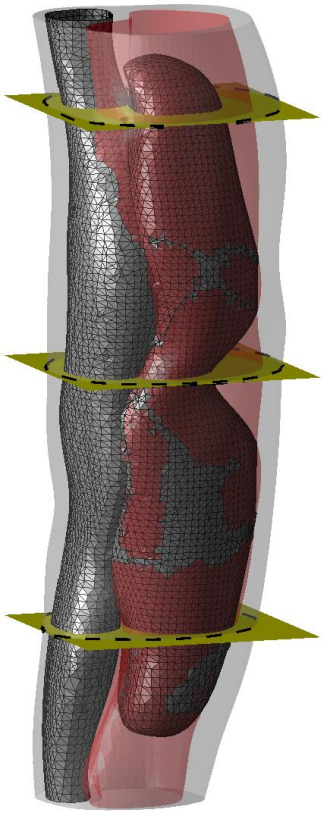

Cross sectional results

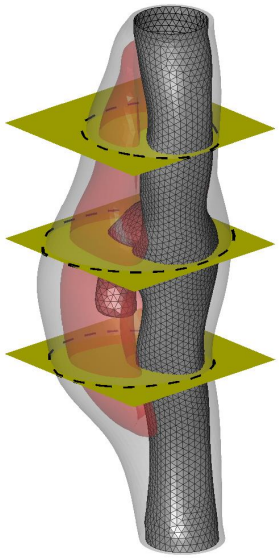

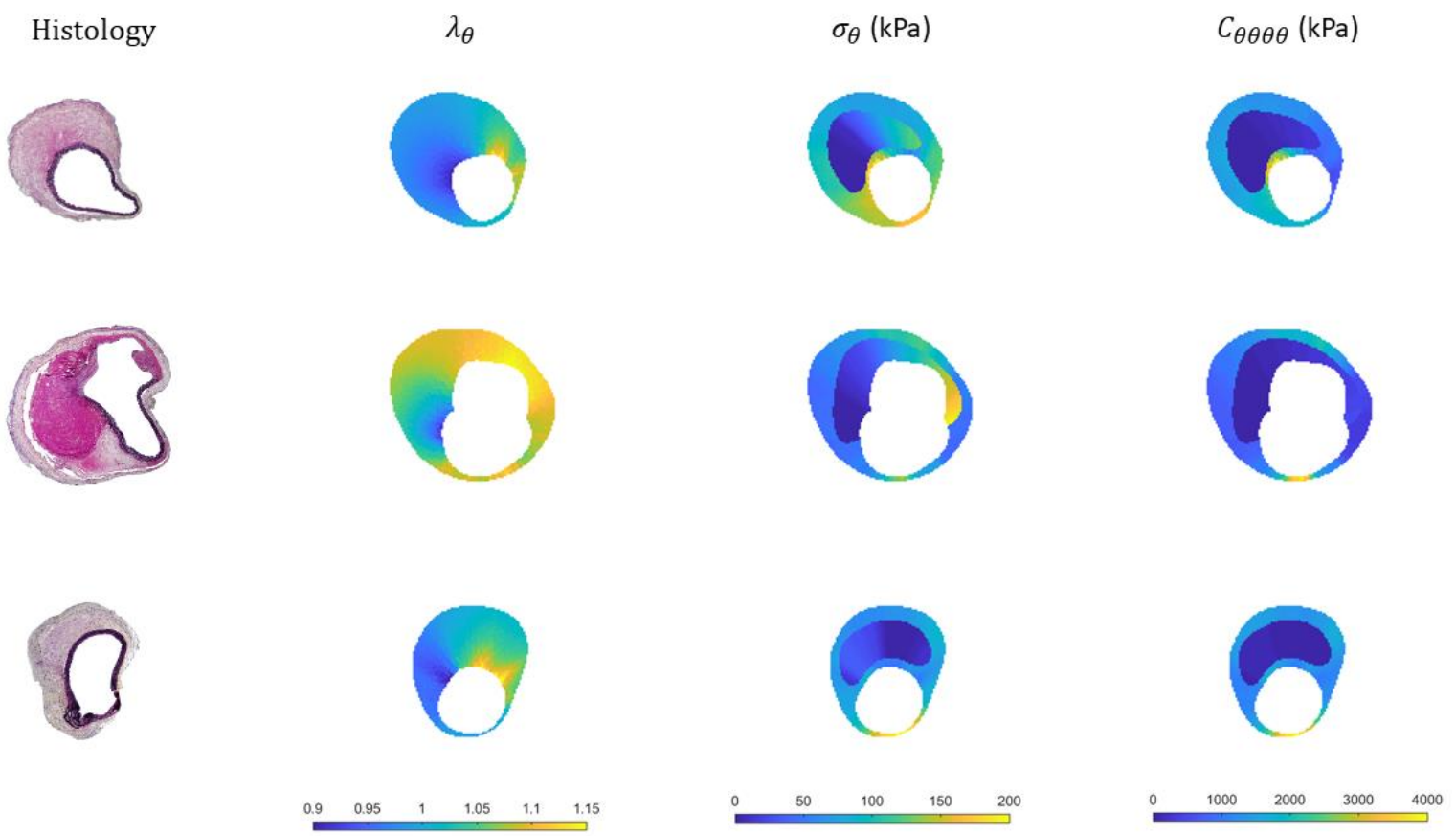

avril@emse.fr

MINES Saint-Étienne

Full-Field Material Parameter Estimation vs thickness distribution

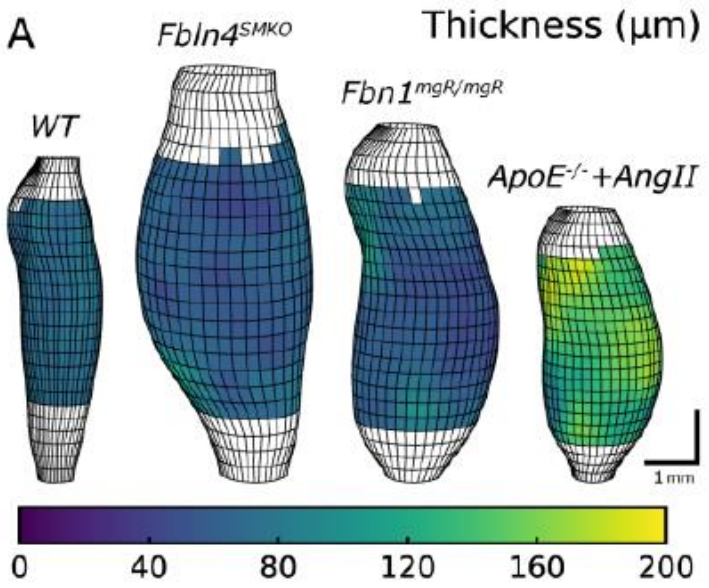

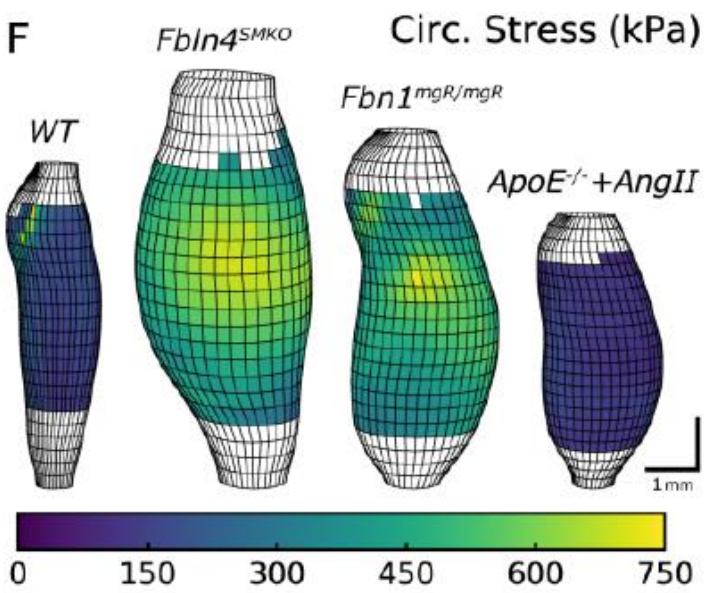

Full-Field Material Parameter Estimation vs local stress

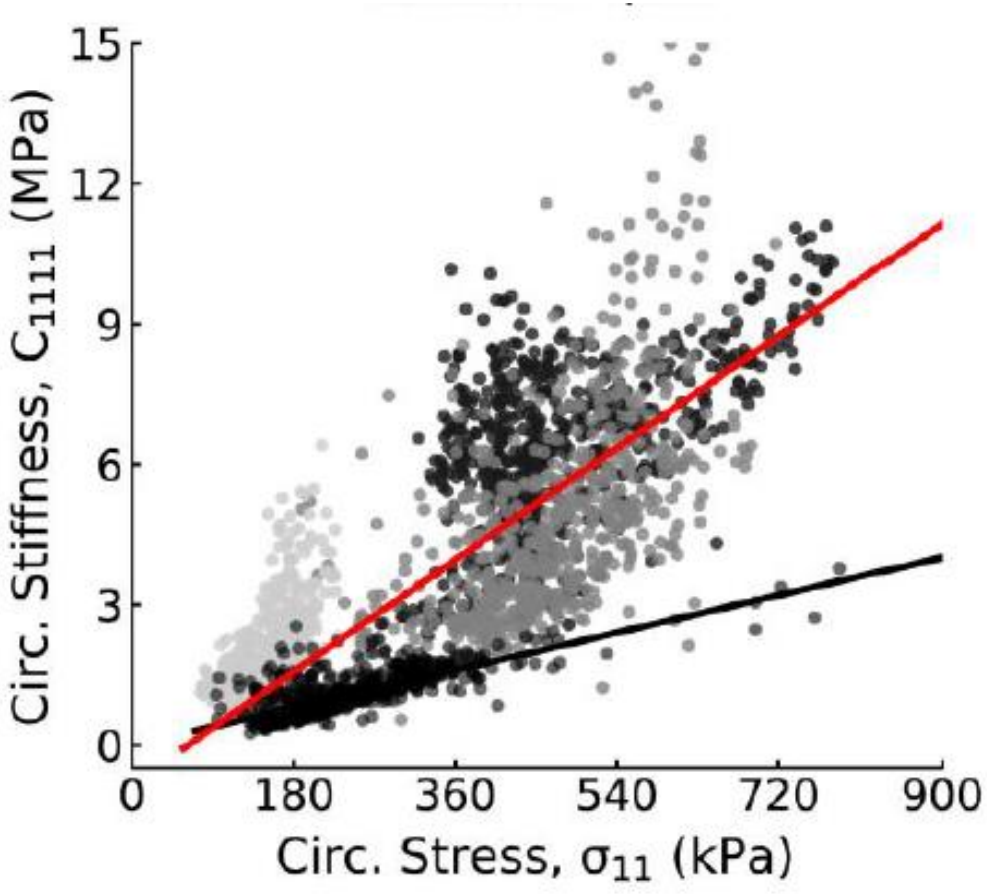

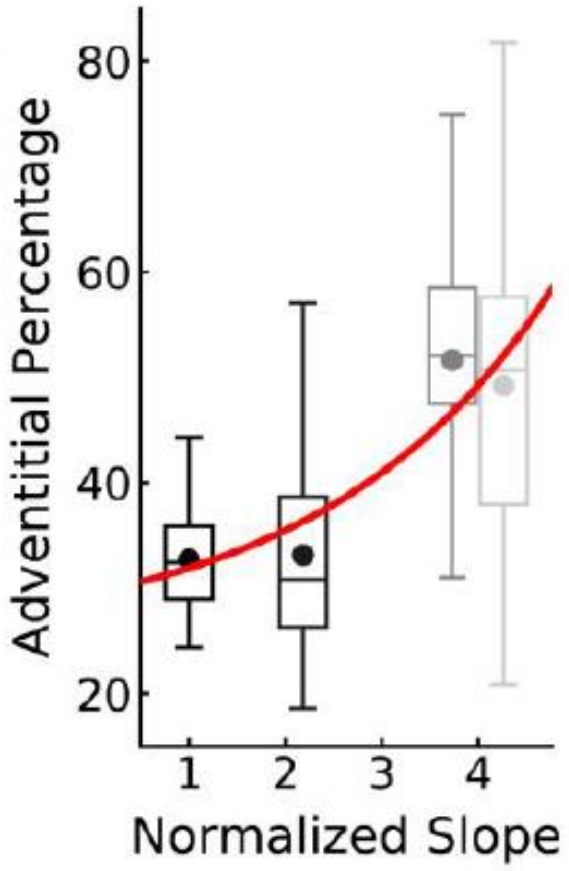

avril@emse.fr

Correlation with tissue µstructure

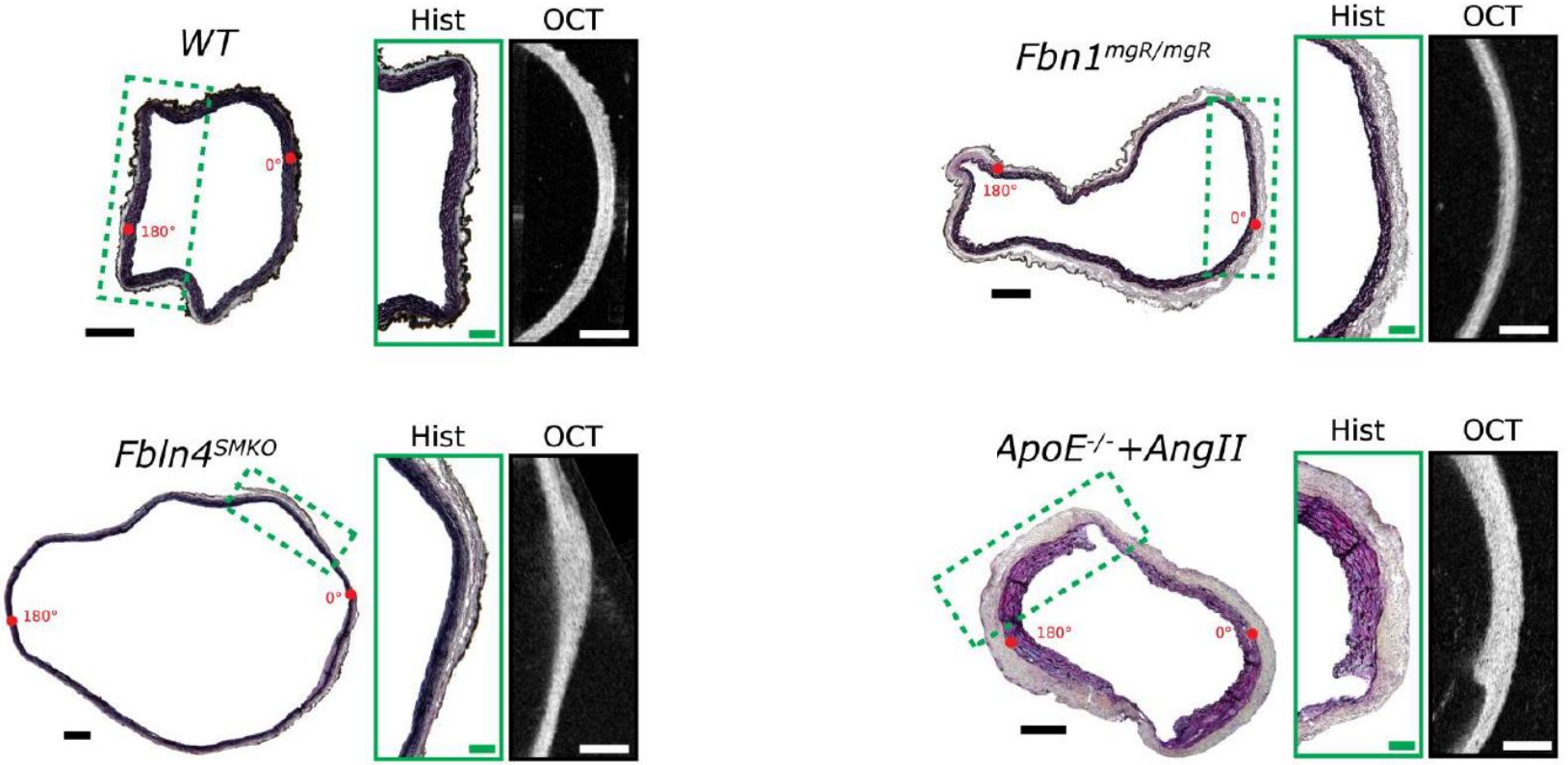

avril@emse.fr

Vision

- **Our vision is that the evolution of the strength and of the wall stress of the aorta during the growth of an aneurysm can be predicted on a patient-specific basis by a computational model.**

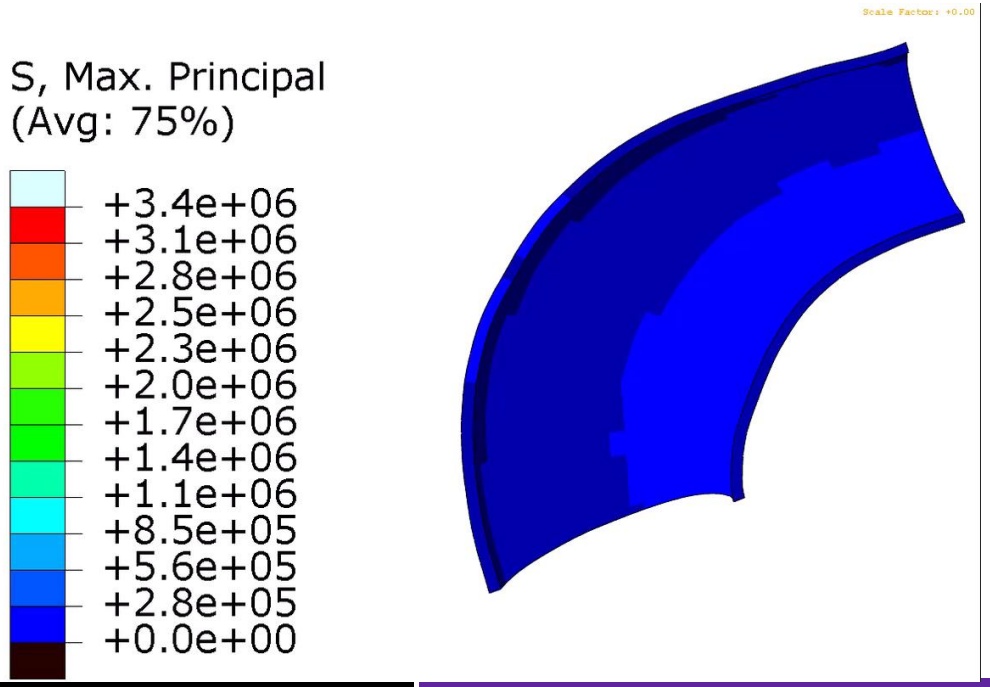

Correlation with flow descriptors

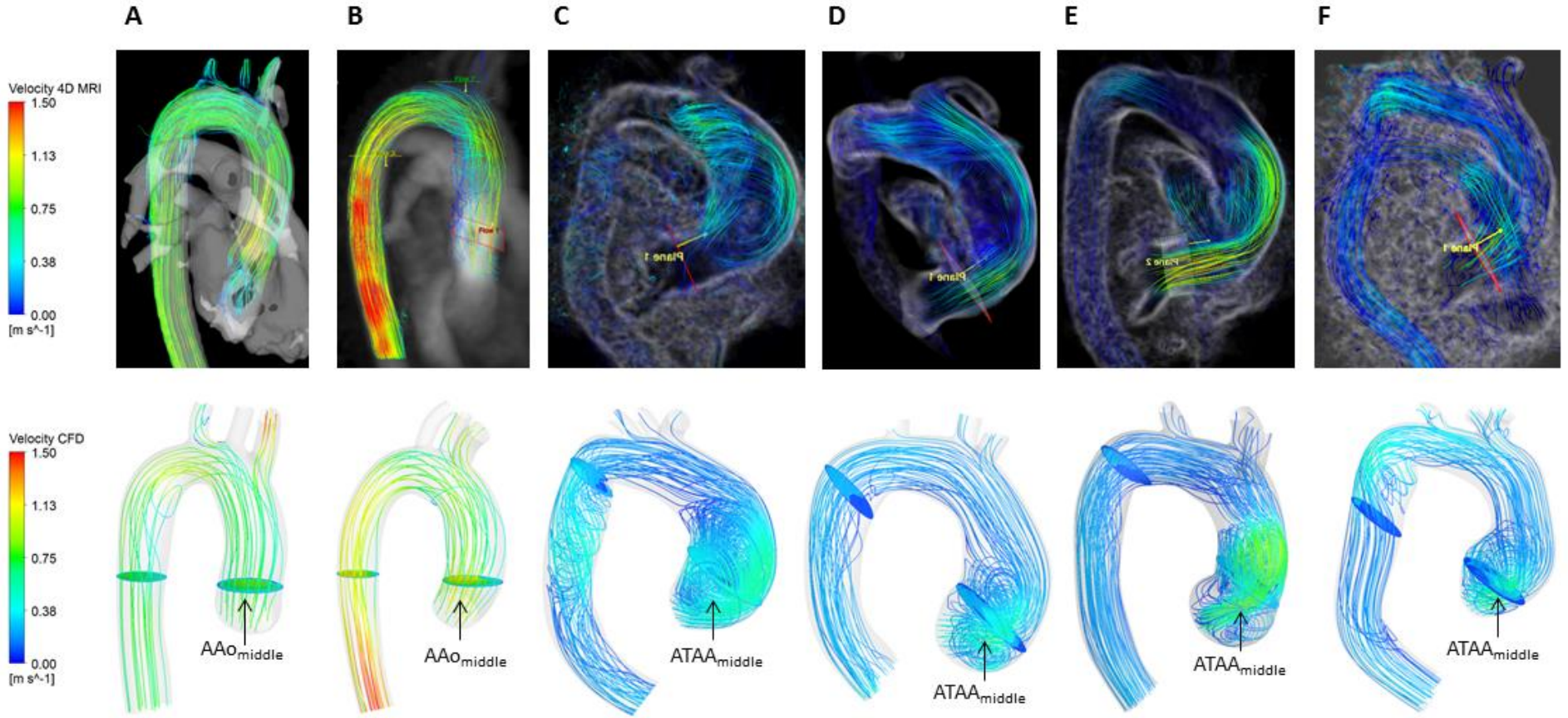

avril@emse.fr

Acknowledgements

- Olfa Trabelsi
- Aaron Romo
- Jin Kim
- Pierre Badel
- Frances Davis
- Victor Acosta
- Jamal Mousavi
- Solmaz Farzeneh
- Francesca Condemi
- Cristina Cavinato
- Jérôme Molimard
- Baptiste Pierrat
- Miguel Angel Gutierrez
- Oscar Alberto Mendoza
- Ambroise Duprey
- Jean-Pierre Favre
- Jean-Noël Albertini
- Salvatore Campisi
- Magalie Viallon
- Pierre Croisille
- Chiara Bellini
- Matthew Bersi
- Jay Humphrey
- Katia Genovese
- Yiqian He
- Di Zuo

Funding:
ERC-2014-CoG BIOLOCHANICS